

AI-Based Synthesis for Complex Human Poses, Motions, and Interactions



Candidate: Georgios Albanis, **Supervisor:** Dr. Konstantinos Kolomvatsos



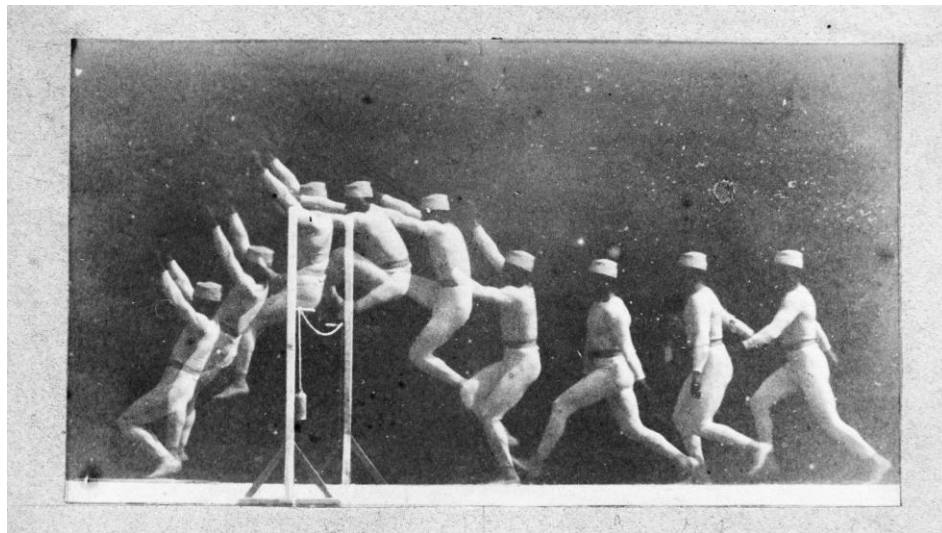


Quote

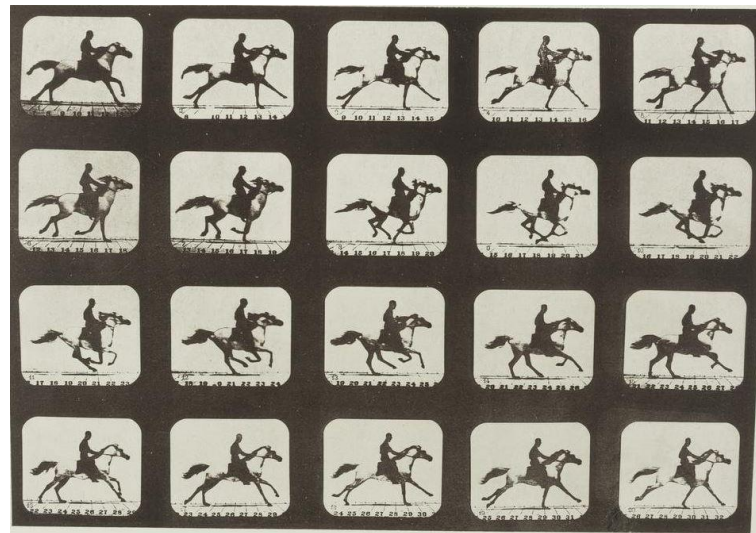




Motion Capture Origins



"The movement of a man jumping hurdle" by Étienne-Jules Marey



"The Horse in Motion" by Eadweard Muybridge





Motion Capture Applications





Existing Solutions



Optical MoCap

High-End Cameras track reflective markers placed on the subject.



IMU MoCap

Inertial Sensors placed on the human body.



Markerless MoCap

No need for sensors based on AI keypoints detections





Existing Solutions

Feature	High-end optical	Low-end optical	Markerless
Cost	•••••	•••	••
Setup effort	•••••	•••	•
Space needs	•••••	•••	•
Cleanup effort	••	•••••	•••••
Data fidelity	•••••	•••	••





The Shift Toward Accessibility

- 💰 Lower CapEx
- 🔧 Lower complexity and expertise needed to operate
- 🖌️ Remove the need for manual cleanup
- 🚫📍 Move to a markerless solution





On what Price?



Lower CapEx → More Noise



Lower complexity and expertise needed to operate



Remove the need for manual cleanup



Move to a markerless solution



→ Improved quality & Maturation

Automation using AI



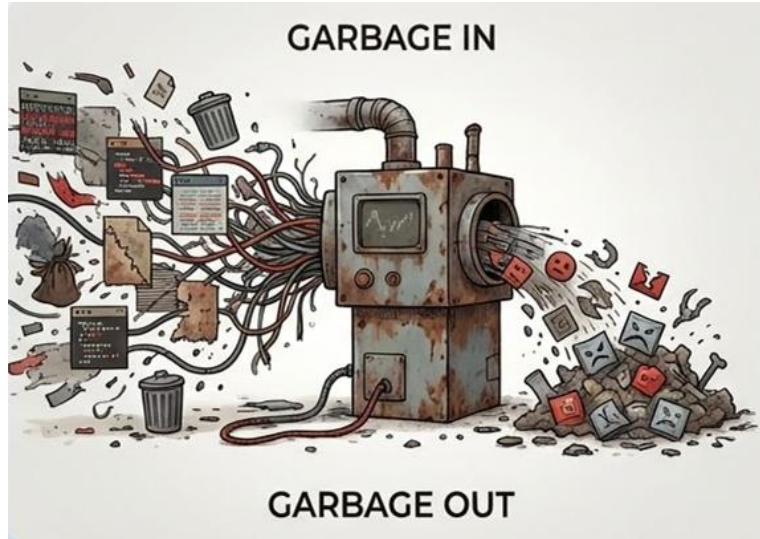


Adversary I - Data Bias



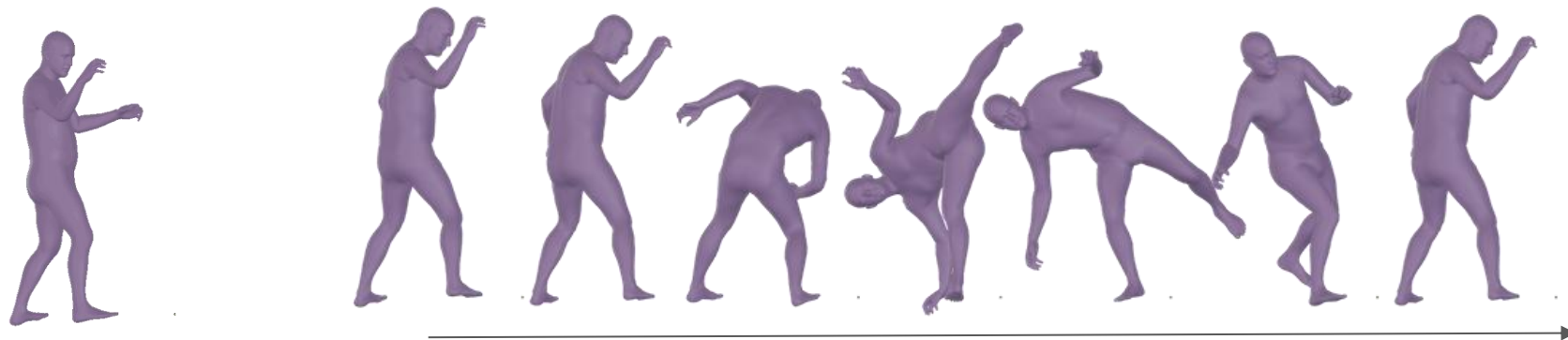


AI Models vs Data





Challenges: Data Redundancy

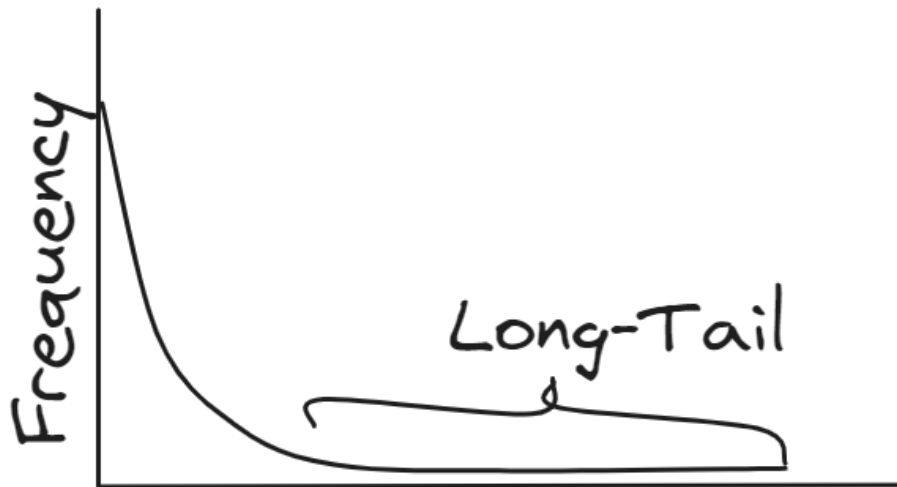


Motion cycle contains similar parts

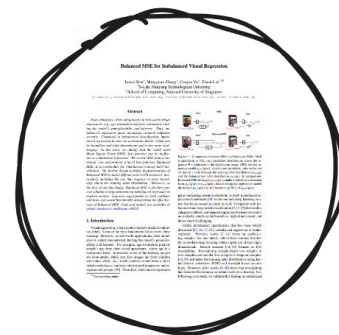




Challenges: Long-tail distribution



Poses

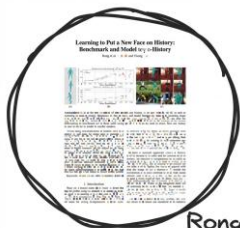
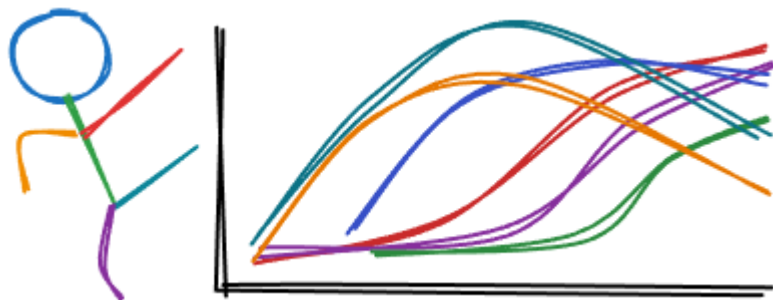


Ren et al.





Challenges: High-dimensionality

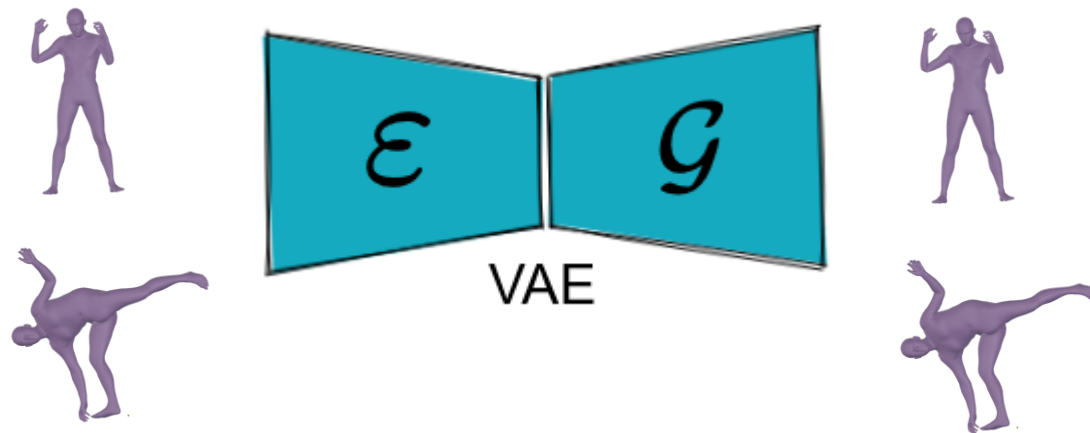


Rong et al.





Representation Learning

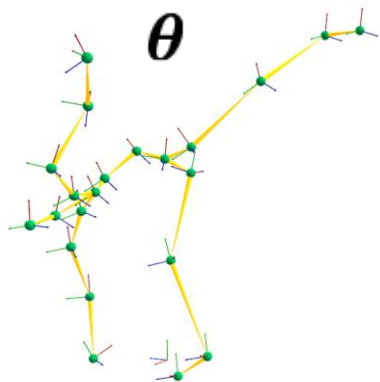


Reflect the bias of the data

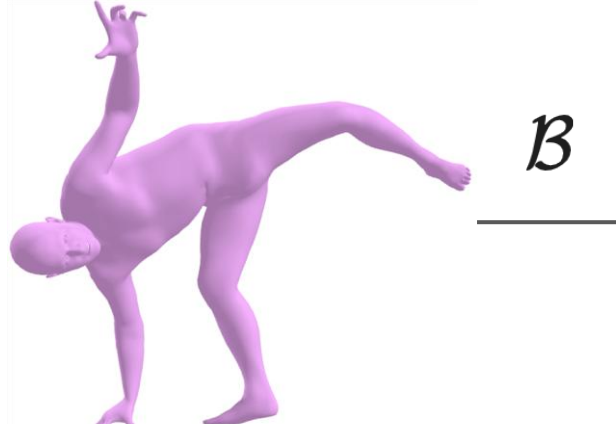
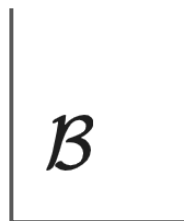
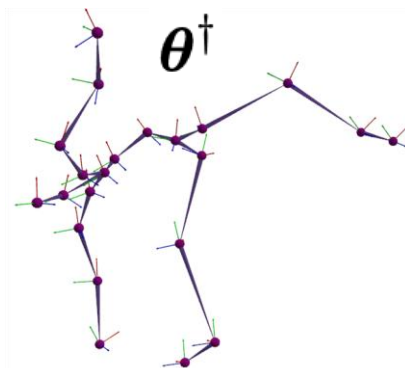




Relevance via Reconstructability

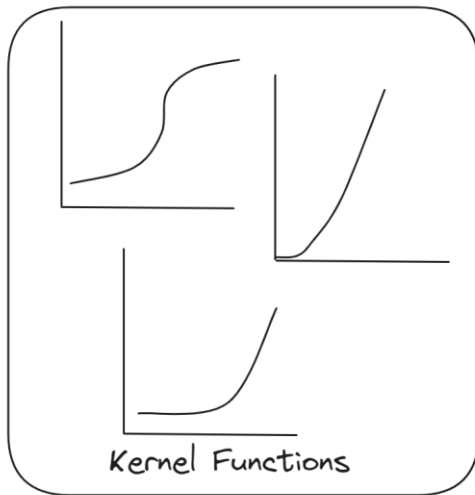


VAE





Relevance via Reconstructability

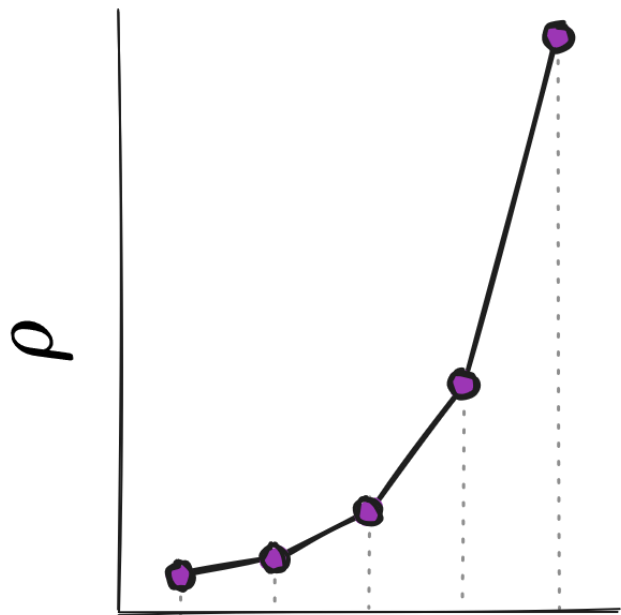


Relevance / Importance





Relevance via Reconstructability



$$\rho * (\mathcal{L}_{JS} + \mathcal{L}_w^v) = \mathcal{L}$$



Overweight the tail samples while training



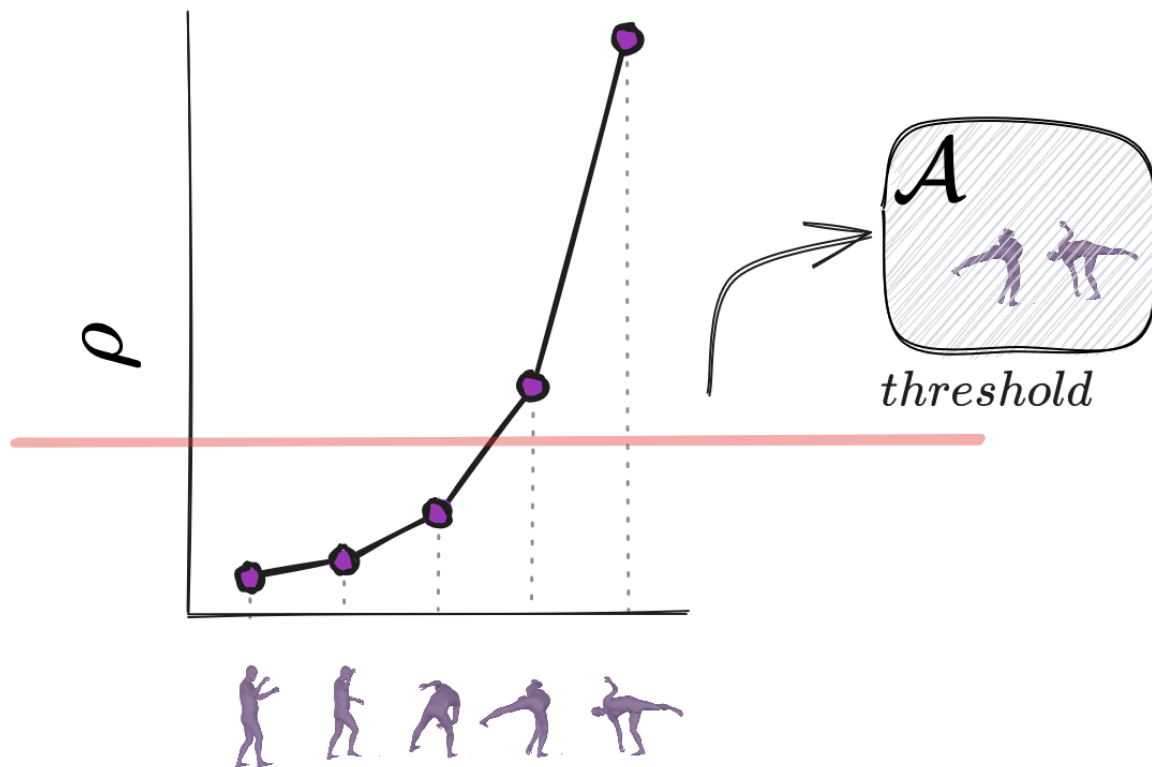


Oversampling using Synthesis





Oversampling using Synthesis

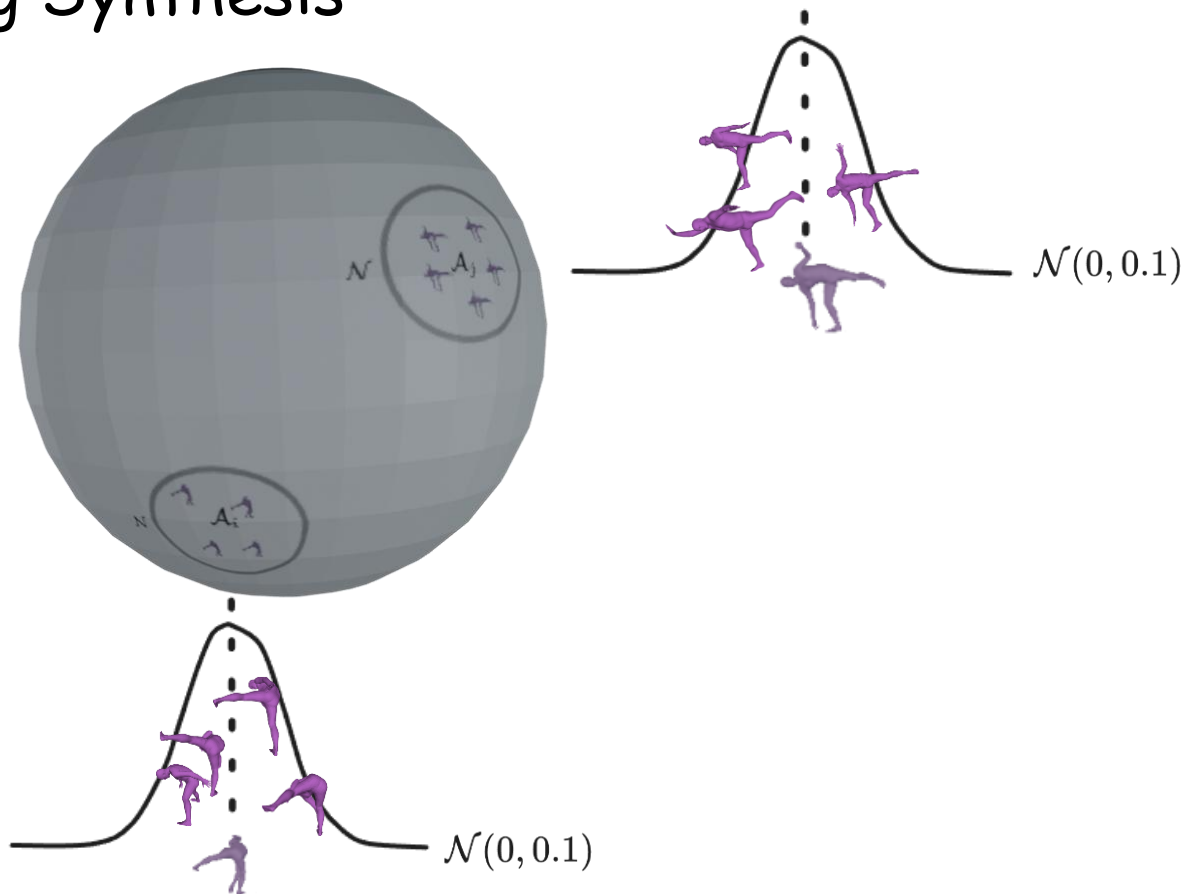




Oversampling using Synthesis

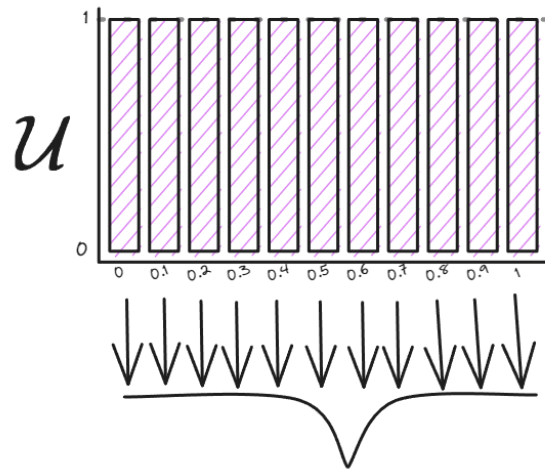


Sample the latent space
around anchors





Oversampling using Synthesis

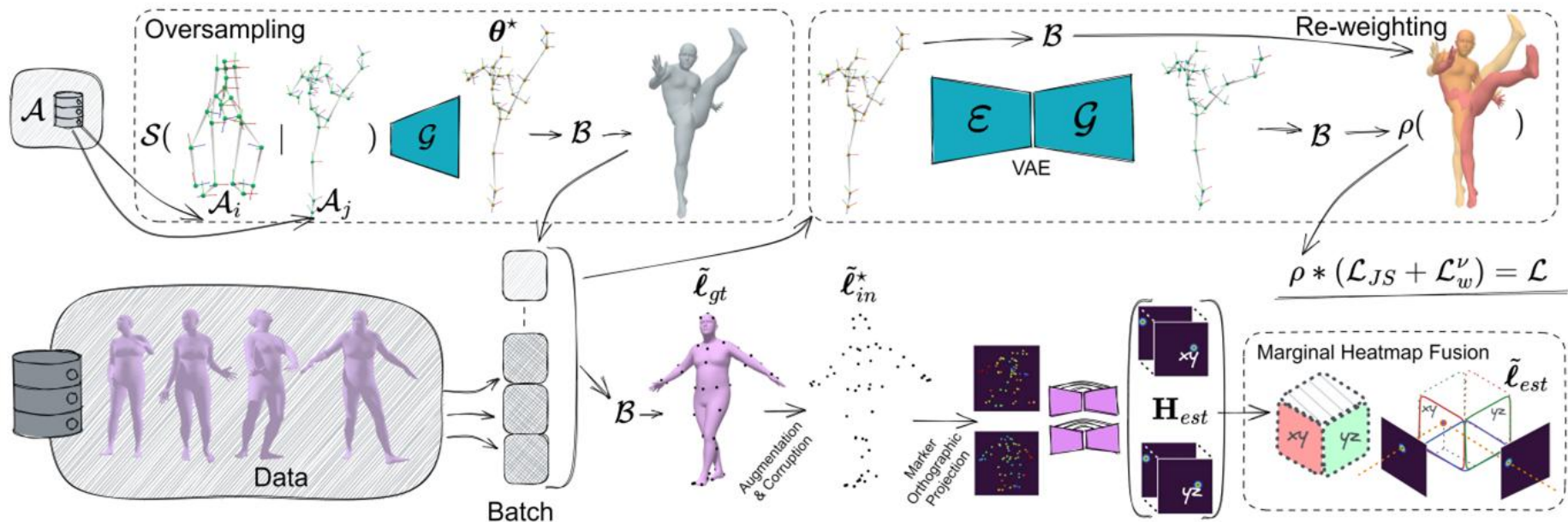


$$\mathcal{S}(\text{pose}_1, \text{pose}_2, b) = \text{pose}_3$$





Training Framework





Results - TAIL dataset

		RMSE ↓	MPJPE ↓	PCK1 ↑			PCK3 ↑			PCK7 ↑		
				all	arms	legs	all	arms	legs	all	arms	legs
	125	36.10 mm	32.60 mm	20.10%	12.13%	23.23%	80.23%	77.10%	80.33%	93.12%	93.43%	94.92%
	13	36.05 mm	32.11 mm	21.01%	13.41%	24.53%	80.12%	77.43%	80.73%	93.23%	93.1%	95.12%
	Ours	35.80 mm	31.15 mm	22.04%	14.99%	25.68%	80.27%	77.94%	81.00%	94.31%	93.%	95.21%
sampling	BMSE	32.90 mm	25.21 mm	27.66%	16.21%	26.13%	81.98%	77.32%	81.10%	94.92%	93.10%	95.10%
	RANDOM	35.80 mm	31.84 mm	23.00%	14.56%	26.01%	81.81%	77.46%	80.20%	95.70%	93.01%	95.30%
	LERP	33.50 mm	28.19 mm	25.02%	12.30%	23.22%	79.82%	76.31%	81.10%	95.22%	93.05%	95.10%
	SLERP	33.25 mm	25.82 mm	24.83%	14.23%	30.29%	80.85%	77.08%	82.16%	95.48%	93.18%	95.75%
	SQUAD	32.68 mm	25.53 mm	25.11%	16.97%	30.35%	83.78%	79.78%	84.15%	95.55%	93.72%	94.63%
	BEZIER	34.01 mm	26.26 mm	24.38%	15.37%	26.14%	82.10%	78.07%	81.34%	95.81%	93.69%	95.66%
	B-spline	34.82 mm	27.49 mm	23.30%	14.53%	24.81%	80.25%	74.84%	81.83%	95.18%	94.02%	95.23%
relevance	e(R)	34.2 mm	26.1 mm	23.10%	12.01%	25.10%	80.88%	74.10%	81.02%	94.95%	93.12%	95.01%
	σ(R)	33.9 mm	26.4 mm	23.61%	12.11%	26.55%	81.00%	74.10%	80.10%	95.21%	93.02%	94.33%
	e(D)	33.81 mm	25.82 mm	25.53%	18.32%	28.67%	81.11%	75.45%	82.84%	94.91%	93.62%	94.93%
	σ(D)	33.79 mm	25.7 mm	22.63%	13.18%	27.27%	79.74%	74.52%	80.40%	95.21%	92.60%	95.45%





Results THuman



		RMSE ↓	MPJPE ↓	PCK1 ↑			PCK3 ↑			PCK7 ↑		
				all	arms	legs	all	arms	legs	all	arms	legs
	125	22.01 mm	17.97 mm	27.15%	19.01%	26.10%	91.45%	87.43%	95.05%	98.01%	97.13%	98.01%
	13	21.81 mm	17.68 mm	28.10%	19.89%	26.55%	91.89%	87.12%	95.11%	98.55%	97.10%	98.49%
	Ours	21.41 mm	17.57 mm	28.69%	21.21%	27.33%	92.08%	87.50%	95.01%	98.59%	97.30%	98.89%
sampling	BMSE	22.21 mm	18.00 mm	25.51%	19.55%	25.02%	91.90%	86.10%	95.05%	98.62%	97.05%	98.15%
	RANDOM	21.52 mm	16.78 mm	31.60%	24.11%	30.11%	92.49%	88.10%	95.11%	98.11%	97.10%	98.95%
	LERP	21.59 mm	16.80 mm	29.48%	21.11%	29.07%	92.68%	88.25%	95.15%	98.58%	97.89%	99.01%
	SLERP	20.43 mm	16.29 mm	30.41%	22.62%	29.02%	93.67%	88.40%	95.32%	98.92%	98.04%	99.05%
	SQUAD	18.80 mm	15.33 mm	32.94%	25.03%	31.20%	94.81%	89.10%	95.41%	99.19%	98.20%	99.31%
	BEZIER	18.94 mm	15.51 mm	32.90%	25.03%	31.23%	94.56%	89.92%	96.15%	99.04%	98.16%	99.22%
	B-spline	20.20 mm	16.06 mm	33.88%	24.78%	36.31%	93.49%	88.47%	94.99%	98.82%	98.07%	98.81%
relevance	e(R)	20.65 mm	16.99 mm	31.11%	22.1%	28.15%	93.01%	88.5%	95.34%	98.55%	97.45%	98.89%
	σ(R)	20.60 mm	16.67 mm	30.99%	22.4%	28.32%	92.79%	88.65%	95.5%	98.61%	97.65%	98.91%
	e(D)	20.83 mm	16.59 mm	31.5%	25.54%	29.18%	93.39%	88.56%	94.75%	98.69%	97.72%	98.76%
	σ(D)	20.49 mm	16.51 mm	31.57%	23.26%	29.35%	92.72%	86.63%	94.84%	98.72%	97.62%	98.95%





Best Sampling



		RMSE ↓	MPJPE ↓	PCK1 ↑			PCK3 ↑			PCK7 ↑		
				all	arms	legs	all	arms	legs	all	arms	legs
sampling	[25]	36.10 mm	32.60 mm	20.10%	12.13%	23.23%	80.23%	77.10%	80.33%	93.12%	93.43%	94.92%
	[13]	36.05 mm	32.11 mm	21.01%	13.41%	24.53%	80.12%	77.43%	80.73%	93.23%	93.1%	95.12%
	Ours	35.80 mm	31.15 mm	22.04%	14.99%	25.68%	80.27%	77.94%	81.00%	94.31%	93.%	95.21%
	BMSE	32.90 mm	25.21 mm	27.66%	16.21%	26.13%	81.98%	77.32%	81.10%	94.92%	93.10%	95.10%
	RANDOM	35.80 mm	31.84 mm	23.00%	14.56%	26.01%	81.81%	77.46%	80.20%	95.70%	93.01%	95.30%
	LERP	33.50 mm	28.19 mm	25.02%	12.30%	23.22%	79.82%	76.31%	81.10%	95.22%	93.05%	95.10%
	SLERP	33.25 mm	25.82 mm	24.83%	14.23%	30.29%	80.85%	77.08%	82.16%	95.48%	93.18%	95.75%
relevance	SQUAD	32.68 mm	25.53 mm	25.11%	16.97%	30.35%	83.78%	79.78%	84.15%	95.55%	93.72%	94.63%
	BEZIER	34.01 mm	26.26 mm	24.38%	15.37%	26.14%	82.10%	78.07%	81.34%	95.81%	93.69%	95.66%
	B-spline	34.82 mm	27.49 mm	23.30%	14.53%	24.81%	80.25%	74.84%	81.83%	95.18%	94.02%	95.23%
	e(R)	34.2 mm	26.1 mm	23.10%	12.01%	25.10%	80.88%	74.10%	81.02%	94.95%	93.12%	95.01%
	σ(R)	33.9 mm	26.4 mm	23.61%	12.11%	26.55%	81.00%	74.10%	80.10%	95.21%	93.02%	94.33%
	e(D)	33.81 mm	25.82 mm	25.53%	18.32%	28.67%	81.11%	75.45%	82.84%	94.91%	93.62%	94.93%
	σ(D)	33.79 mm	25.7 mm	22.63%	13.18%	27.27%	79.74%	74.52%	80.40%	95.21%	92.60%	95.45%





Best Sampling



$SLERP(A_i, A_j)$



$SQUAD(A_i, A_j, A_k, A_l)$





Best Relevance

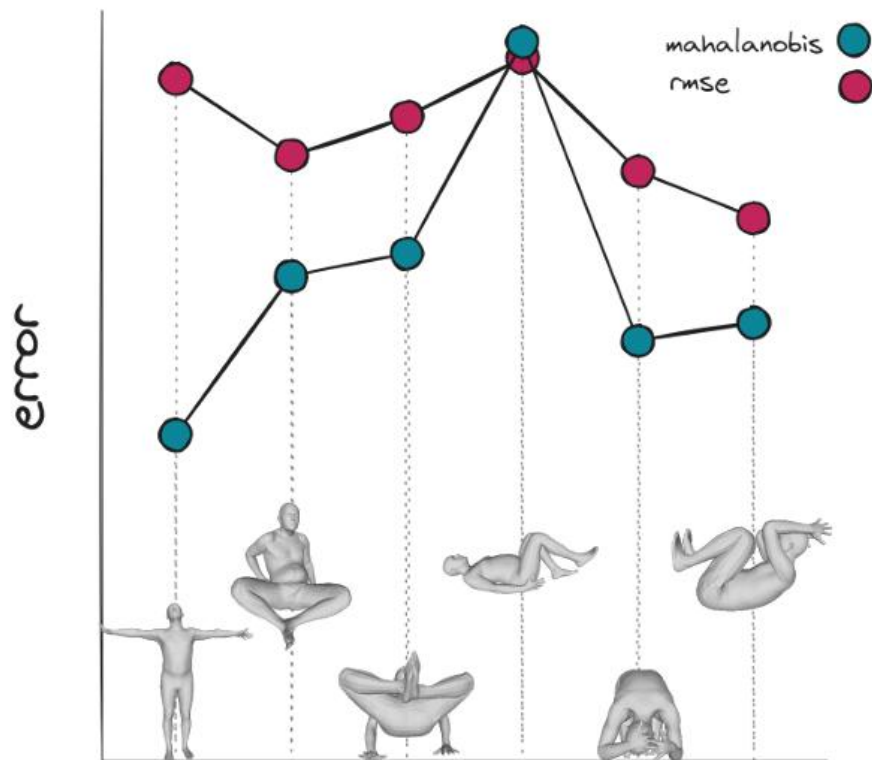


		RMSE ↓	MPJPE ↓	PCK1 ↑			PCK3 ↑			PCK7 ↑		
				all	arms	legs	all	arms	legs	all	arms	legs
	125	36.10 mm	32.60 mm	20.10%	12.13%	23.23%	80.23%	77.10%	80.33%	93.12%	93.43%	94.92%
	13	36.05 mm	32.11 mm	21.01%	13.41%	24.53%	80.12%	77.43%	80.73%	93.23%	93.1%	95.12%
	Ours	35.80 mm	31.15 mm	22.04%	14.99%	25.68%	80.27%	77.94%	81.00%	94.31%	93.%	95.21%
sampling	BMSE	32.90 mm	25.21 mm	27.66%	16.21%	26.13%	81.98%	77.32%	81.10%	94.92%	93.10%	95.10%
	RANDOM	35.80 mm	31.84 mm	23.00%	14.56%	26.01%	81.81%	77.46%	80.20%	95.70%	93.01%	95.30%
	LERP	33.50 mm	28.19 mm	25.02%	12.30%	23.22%	79.82%	76.31%	81.10%	95.22%	93.05%	95.10%
	SLERP	33.25 mm	25.82 mm	24.83%	14.23%	30.29%	80.85%	77.08%	82.16%	95.48%	93.18%	95.75%
	SQUAD	32.68 mm	25.53 mm	25.11%	16.97%	30.35%	83.78%	79.78%	84.15%	95.55%	93.72%	94.63%
	BEZIER	34.01 mm	26.26 mm	24.38%	15.37%	26.14%	82.10%	78.07%	81.34%	95.81%	93.69%	95.66%
	B-spline	34.82 mm	27.49 mm	23.30%	14.53%	24.81%	80.25%	74.84%	81.83%	95.18%	94.02%	95.23%
relevance	e(R)	34.2 mm	26.1 mm	23.10%	12.01%	25.10%	80.88%	74.10%	81.02%	94.95%	93.12%	95.01%
	σ(R)	33.9 mm	26.4 mm	23.61%	12.11%	26.55%	81.00%	74.10%	80.10%	95.21%	93.02%	94.33%
	e(D)	33.81 mm	25.82 mm	25.53%	18.32%	28.67%	81.11%	75.45%	82.84%	94.91%	93.62%	94.93%
	σ(D)	33.79 mm	25.7 mm	22.63%	13.18%	27.27%	79.74%	74.52%	80.40%	95.21%	92.60%	95.45%





Best Relevance





Synergistically



		RMSE ↓	MPJPE ↓	PCK1 ↑			PCK3 ↑			PCK7 ↑		
				all	arms	legs	all	arms	legs	all	arms	legs
	[25]	36.10 mm	32.60 mm	20.10%	12.13%	23.23%	80.23%	77.10%	80.33%	93.12%	93.43%	94.92%
	[13]	36.05 mm	32.11 mm	21.01%	13.41%	24.53%	80.12%	77.43%	80.73%	93.23%	93.1%	95.12%
	Ours	35.80 mm	31.15 mm	22.04%	14.99%	25.68%	80.27%	77.94%	81.00%	94.31%	93.%	95.21%
sampling	BMSE	32.90 mm	25.21 mm	27.66%	16.21%	26.13%	81.98%	77.32%	81.10%	94.92%	93.10%	95.10%
	RANDOM	35.80 mm	31.84 mm	23.00%	14.56%	26.01%	81.81%	77.46%	80.20%	95.70%	93.01%	95.30%
	LERP	33.50 mm	28.19 mm	25.02%	12.30%	23.22%	79.82%	76.31%	81.10%	95.22%	93.05%	95.10%
	SLERP	33.25 mm	25.82 mm	24.83%	14.23%	30.29%	80.85%	77.08%	82.16%	95.48%	93.18%	95.75%
	SQUAD	32.68 mm	25.53 mm	25.11%	16.97%	30.35%	83.78%	79.78%	84.15%	95.55%	93.72%	94.63%
	BEZIER	34.01 mm	26.26 mm	24.38%	15.37%	26.14%	82.10%	78.07%	81.34%	95.81%	93.69%	95.66%
	B-spline	34.82 mm	27.49 mm	23.30%	14.53%	24.81%	80.25%	74.84%	81.83%	95.18%	94.02%	95.23%
relevance	e(R)	34.2 mm	26.1 mm	23.10%	12.01%	25.10%	80.88%	74.10%	81.02%	94.95%	93.12%	95.01%
	σ(R)	33.9 mm	26.4 mm	23.61%	12.11%	26.55%	81.00%	74.10%	80.10%	95.21%	93.02%	94.33%
	e(D)	33.81 mm	25.82 mm	25.53%	18.32%	28.67%	81.11%	75.45%	82.84%	94.91%	93.62%	94.93%
	σ(D)	33.79 mm	25.7 mm	22.63%	13.18%	27.27%	79.74%	74.52%	80.40%	95.21%	92.60%	95.45%
ortho	e(D) + SQUAD	34.06 mm	26.59 mm	25.21%	14.28%	30.16%	82.78%	78.21%	83.33%	95.80%	95.94%	95.35%
	σ(D) + SQUAD	32.54 mm	24.48 mm	28.15%	18.90%	29.68%	83.89%	79.85%	82.90%	95.54%	95.60%	94.33%





Results - TAIL dataset

		RMSE ↓	MPJPE ↓	PCK1 ↑			PCK3 ↑			PCK7 ↑		
				all	arms	legs	all	arms	legs	all	arms	legs
	[125]	36.10 mm	32.60 mm	20.10%	12.13%	23.23%	80.23%	77.10%	80.33%	93.12%	93.43%	94.92%
	[13]	36.05 mm	32.11 mm	21.01%	13.41%	24.53%	80.12%	77.43%	80.73%	93.23%	93.1%	95.12%
	Ours	35.80 mm	31.15 mm	22.04%	14.99%	25.68%	80.27%	77.94%	81.00%	94.31%	93%	95.21%
sampling	BMSE	32.80 mm	25.21 mm	27.66%	16.21%	26.13%	81.98%	77.30%	81.10%	94.92%	93.10%	95.10%
	RANDOM	35.80 mm	31.84 mm	23.00%	14.56%	26.01%	81.81%	77.46%	80.20%	95.70%	93.01%	95.30%
	LERP	33.80 mm	28.19 mm	25.02%	12.30%	23.22%	79.82%	75.10%	81.0%	95.22%	93.05%	95.10%
	SLERP	33.80 mm	25.82 mm	24.83%	14.23%	30.29%	82.35%	77.00%	82.1%	95.48%	93.18%	95.75%
	SQUAD	32.60 mm	25.3 mm	25.11%	16.97%	30.35%	83.78%	79.70%	81.1%	95.55%	93.72%	94.63%
	BEZIER	34.01 mm	26.26 mm	24.38%	15.37%	26.14%	82.10%	78.07%	81.1%	95.81%	93.69%	95.66%
	B-spline	34.82 mm	27.49 mm	23.30%	14.53%	24.81%	80.25%	74.84%	81.83%	95.18%	94.02%	95.23%
relevance	e(R)	34.2 mm	26.1 mm	23.10%	12.01%	25.10%	80.88%	74.10%	81.02%	94.95%	93.12%	95.01%
	σ(R)	33.9 mm	26.4 mm	23.61%	12.11%	26.55%	81.00%	74.10%	80.10%	95.21%	93.02%	94.33%
	e(D)	33.81 mm	25.82 mm	25.53%	18.32%	28.67%	81.11%	75.45%	82.84%	94.91%	93.62%	94.93%
	σ(D)	33.79 mm	25.7 mm	22.63%	13.18%	27.27%	79.74%	74.52%	80.40%	95.21%	92.60%	95.45%
ortho	e(D) + SQUAD	34.06 mm	26.59 mm	25.21%	14.28%	30.16%	82.78%	78.21%	83.33%	95.80%	95.94%	95.35%
	σ(D) + SQUAD	32.54 mm	24.48 mm	28.15%	18.90%	29.68%	83.89%	79.85%	82.90%	95.54%	95.60%	94.33%





Results - TAIL dataset

		RMSE ↓	MPJPE ↓	PCK1 ↑			PCK3 ↑			PCK7 ↑		
				all	arms	legs	all	arms	legs	all	arms	legs
	125	36.10 mm	32.60 mm	20.10%	12.13%	23.23%	80.23%	77.10%	80.33%	93.12%	93.43%	94.92%
	13	36.05 mm	32.11 mm	21.01%	13.41%	24.53%	80.12%	77.43%	80.73%	93.23%	93.1%	95.12%
	Ours	35.80 mm	31.15 mm	22.04%	14.99%	25.68%	80.27%	77.94%	81.00%	94.31%	93.%	95.21%
sampling	BMSE	32.90 mm	25.21 mm	27.66%	16.21%	26.13%	81.98%	77.32%	81.10%	94.92%	93.10%	95.10%
	RANDOM	35.80 mm	31.84 mm	23.00%	14.56%	26.01%	81.81%	77.46%	80.0%	95.70%	93.01%	95.30%
	LERP	33.8 mm	29.19 mm	25.02%	12.30%	23.22%	79.82%	76.31%	80.0%	95.2%	93.05%	95.10%
	SLERP	33.8 mm	25.82 mm	24.83%	14.23%	30.29%	80.88%	77.08%	80.0%	95.48%	93.18%	95.75%
	SQUAD	34.0 mm	25.53 mm	25.11%	16.97%	30.35%	83.78%	77.0%	80.0%	95.55%	93.72%	94.63%
	BEZIER	34.0 mm	26.26 mm	24.38%	15.37%	26.14%	82.10%	78.07%	81.34%	95.81%	93.69%	95.66%
	B-spline	34.0 mm	27.49 mm	23.30%	14.53%	24.81%	80.25%	74.84%	81.83%	95.18%	94.02%	95.23%
relevance	e(R)	34.0 mm	26.1 mm	23.10%	12.01%	25.10%	80.88%	74.10%	81.02%	94.95%	93.12%	95.01%
	σ(R)	33.8 mm	26.4 mm	23.61%	12.11%	26.55%	81.00%	74.10%	80.10%	95.21%	93.02%	94.33%
	e(D)	33.8 mm	25.82 mm	25.53%	18.32%	28.67%	81.11%	75.45%	82.84%	94.91%	93.62%	94.93%
	σ(D)	33.79 mm	25.7 mm	22.63%	13.18%	27.27%	79.74%	74.52%	80.40%	95.21%	92.60%	95.45%
ortho	e(D) + SQUAD	34.06 mm	26.59 mm	25.21%	14.28%	30.16%	82.78%	78.21%	83.33%	95.80%	95.94%	95.35%
	σ(D)+ SQUAD	32.54 mm	24.48 mm	28.15%	18.90%	29.68%	83.89%	79.85%	82.90%	95.54%	95.60%	94.33%





Results - TAIL dataset

		RMSE ↓	MPJPE ↓	PCK1 ↑			PCK3 ↑			PCK7 ↑		
				all	arms	legs	all	arms	legs	all	arms	legs
	125	36.10 mm	32.60 mm	20.10%	12.13%	23.23%	80.23%	77.10%	80.33%	93.12%	93.43%	94.92%
	13	36.05 mm	32.11 mm	21.01%	13.41%	24.53%	80.12%	77.43%	80.73%	93.23%	93.1%	95.12%
	Ours	35.80 mm	31.15 mm	22.04%	14.99%	25.68%	80.27%	77.94%	81.00%	94.31%	93.%	95.21%
sampling	BMSE	32.90 mm	27.21 mm	27.66%	16.21%	26.13%	81.98%	77.32%	81.10%	94.92%	93.10%	95.10%
	RANDOM	35.80 mm	34 mm	23.00%	14.56%	26.01%	81.81%	77.46%	80.5%	95.70%	93.01%	95.30%
	LERP	33.50 mm	31 mm	25.02%	12.30%	23.22%	79.82%	76.31%	81.1%	95.22%	93.05%	95.10%
	SLERP	33.25 mm	31 mm	24.83%	14.23%	30.29%	80.85%	77.08%	81.1%	95.48%	93.18%	95.75%
	SQUAD	32.68 mm	27 mm	25.11%	16.97%	30.35%	83.78%	79.78%	81.1%	95.55%	93.72%	94.63%
	BEZIER	34.01 mm	26 mm	24.38%	15.37%	26.14%	82.10%	78.07%	81.1%	95.81%	93.69%	95.66%
	B-spline	34.82 mm	29 mm	23.30%	14.53%	24.81%	80.25%	74.84%	81.1%	95.18%	94.02%	95.23%
relevance	e(R)	34.2 mm	21 mm	23.10%	12.01%	25.10%	80.88%	74.10%	81.1%	94.95%	93.12%	95.01%
	σ(R)	33.9 mm	24 mm	23.61%	12.11%	26.55%	81.00%	74.10%	80.1%	95.21%	93.02%	94.33%
	e(D)	33.81 mm	28.82 mm	25.53%	18.32%	28.67%	81.11%	75.45%	82.8%	94.91%	93.62%	94.93%
	σ(D)	33.79 mm	27 mm	22.63%	13.18%	27.27%	79.74%	74.52%	80.4%	95.21%	92.60%	95.45%
ortho	e(D) + SQUAD	34.06 mm	26.59 mm	25.21%	14.28%	30.16%	82.78%	78.21%	83.33%	95.80%	95.94%	95.35%
	σ(D)+ SQUAD	32.54 mm	24.48 mm	28.15%	18.90%	29.68%	83.89%	79.85%	82.90%	95.54%	95.60%	94.33%





Results - Different Model Architecture

		RMSE ↓	MPJPE ↓	PCK1 ↑	PCK3 ↑	PCK7 ↑
TH2	[13]	21.81 <i>mm</i>	17.68 <i>mm</i>	28.10%	91.89%	98.55%
	[13] + BMSE	22.01 <i>mm</i>	18.05 <i>mm</i>	25.05%	91.79%	98.65%
	[13] + Ours	19.95 <i>mm</i>	16.45 <i>mm</i>	32.30%	92.45%	98.70%
TAIL	[13]	36.05 <i>mm</i>	32.11 <i>mm</i>	21.01%	80.12%	93.23%
	[13] + BMSE	33.34 <i>mm</i>	26.15 <i>mm</i>	25.35%	81.03%	93.52%
	[13] + Ours	33.01 <i>mm</i>	25.55 <i>mm</i>	24.99%	82.75%	93.90%
GENE	[13]	190.32 <i>mm</i>	105.33 <i>mm</i>	28.01%	59.92%	73.45%
	[13] + BMSE	150.15 <i>mm</i>	101.01 <i>mm</i>	28.50%	60.01%	74.65%
	[13] + Ours	110.01 <i>mm</i>	70.55 <i>mm</i>	30.15%	62.75%	80.05%





Results - Different VAE

		RMSE ↓	MPJPE ↓	PCK1 ↑	PCK3 ↑	PCK7 ↑
TH2	Benchmark	21.41 <i>mm</i>	17.57 <i>mm</i>	28.69%	92.08%	98.59%
	Benchmark + [4]	19.01 <i>mm</i>	16.55 <i>mm</i>	31.11%	93.33%	98.85%
	Benchmark + Ours	18.69 <i>mm</i>	15.20 <i>mm</i>	35.59%	94.53%	99.09%
TAIL	Benchmark	35.80 <i>mm</i>	31.15 <i>mm</i>	22.04%	80.27%	94.31%
	Benchmark + [4]	33.45 <i>mm</i>	26.01 <i>mm</i>	24.35%	82.03%	94.25%
	Benchmark + Ours	32.54 <i>mm</i>	24.48 <i>mm</i>	25.15%	83.29%	95.54%
GENE	Benchmark	170.31 <i>mm</i>	103.83 <i>mm</i>	29.04%	60.91%	73.85%
	Benchmark + [4]	125.15 <i>mm</i>	75.55 <i>mm</i>	30.01%	61.01%	75.65%
	Benchmark + Ours	108.74 <i>mm</i>	65.33 <i>mm</i>	31.52%	62.85%	81.48%





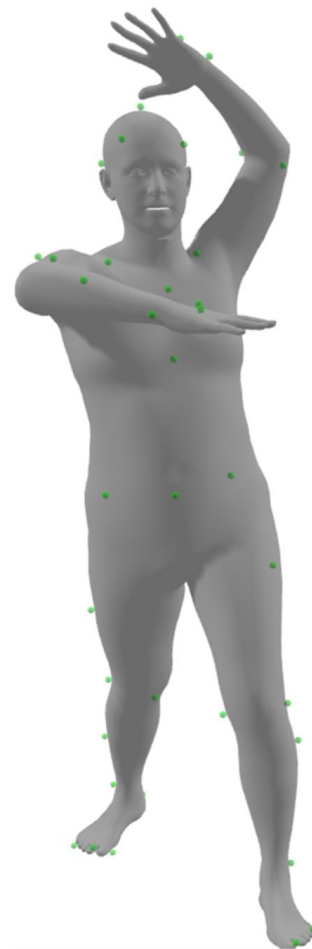
Adversary II - Noise





Model Noise

AI model -> information noise
(certain -> uncertain predictions)



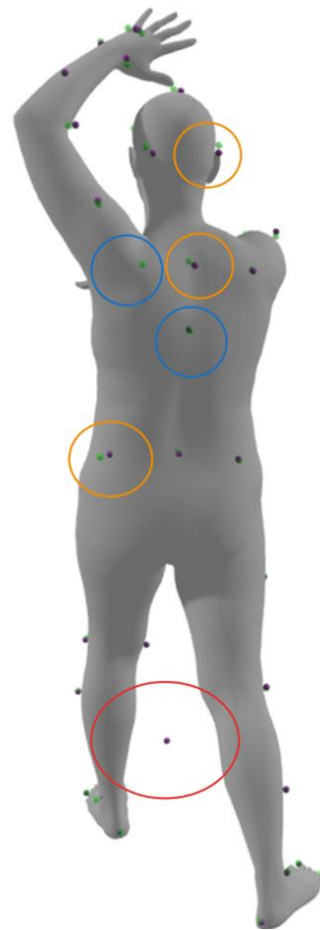


Signal Noise

Low-cost sensors ->

noisy inputs & intense ghosting

Sparse views -> missing information





Non-linear optimization

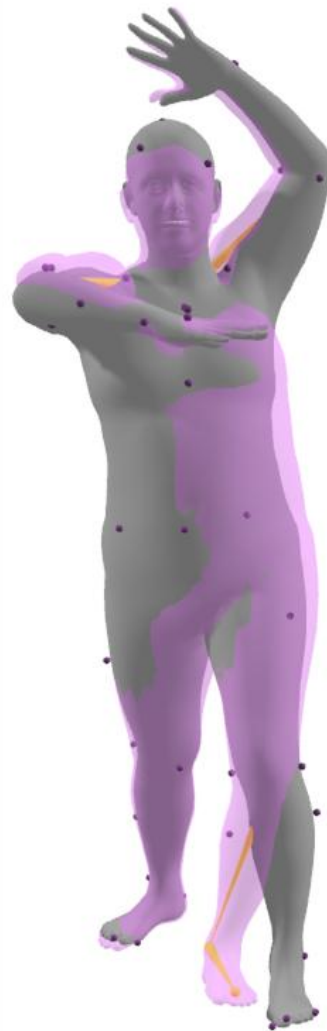
Result is affected by the different sources of noise



Mahmood et al.



Loper et al.





Robust Estimators

Robust Smoothing

Huber et al.

Abstract: This chapter reviews robust smoothing. When a curve is sampled without repetition at discrete points, and the measurement contains observational errors, does a smoothing procedure exist which is linear, is the best for any noise, consistently converges, whose asymptotic behavior is optimal, and provides more insight by analyzing random functions. It is found that the best procedure is the Huber and Wang procedure, which is a natural extension of the data. This can be achieved in a number of ways for least smoothing in a more arbitrary fashion, then choosing one that performs best to match them on smoothed curves, and finally smoothing again, however, both the performance and the subtle effects of such an approach are difficult to appraise.

Huber et al.

Introduction to Bayesian Image Analysis

H. H. Swanson

Abstract: This review explores the fundamentals of Bayesian analysis as applied to image processing and computer vision. The Bayesian approach to probability and data analysis is introduced, with emphasis on its utility for accurate statistics, and the integration of prior knowledge. The discussion covers the use of Bayes' theorem, likelihoods, and four techniques to large problems in image reconstruction that make use of sophisticated prior information.

Hanson et al.

A Generalized Adaptive Kernel Line Detector

Barron et al.

Abstract: This paper presents a new method for detecting lines in images. The method is based on a generalized adaptive kernel line detector. The detector is able to detect lines of arbitrary orientation and width. The method is robust to noise and clutter. The detector is able to detect lines in images with varying contrast and background. The method is able to detect lines in images with varying scale and resolution. The detector is able to detect lines in images with varying orientation and width. The method is able to detect lines in images with varying contrast and background. The detector is able to detect lines in images with varying scale and resolution. The method is able to detect lines in images with varying orientation and width.

Barron et al.

- Known distribution
- Intensive tuning
- Require confidence knowledge





Noise-aware solver

Adaptive fitting

- optimize for the observations/estimations' uncertainty region

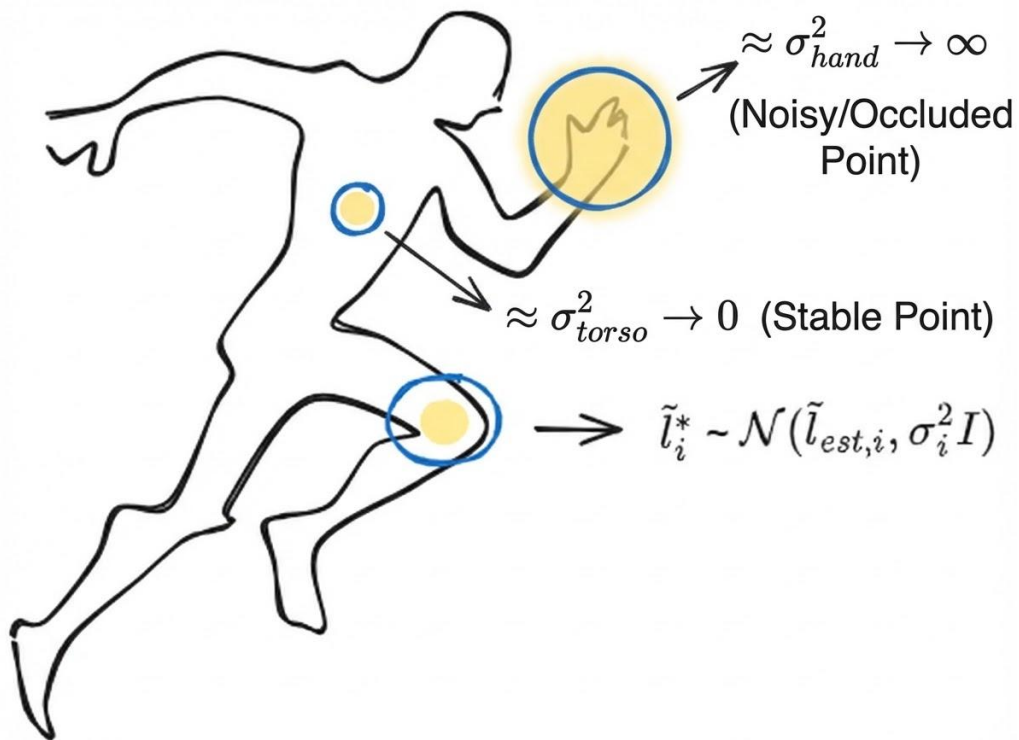
$$E_{data} = \sum_i^L \frac{1}{2\sigma_i^2} \|\tilde{\ell}_{est,i} - \tilde{\ell}_i^*\|_2 + \log \sigma_i$$

Different weights for each landmark





Noise Modelling

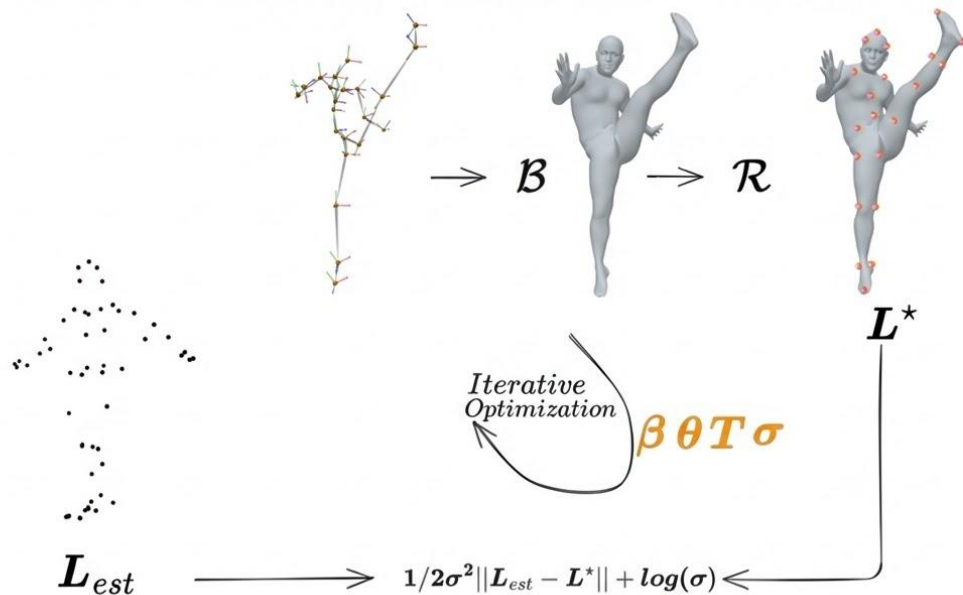


- Separate noise distribution
- Each landmark has its own variance





Noise-aware solver



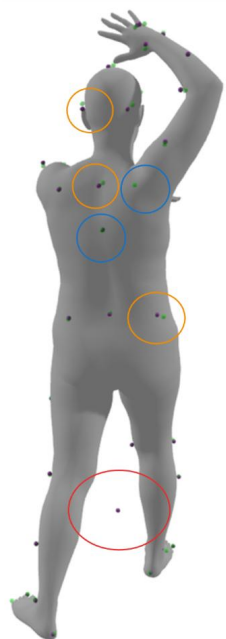


Experiments



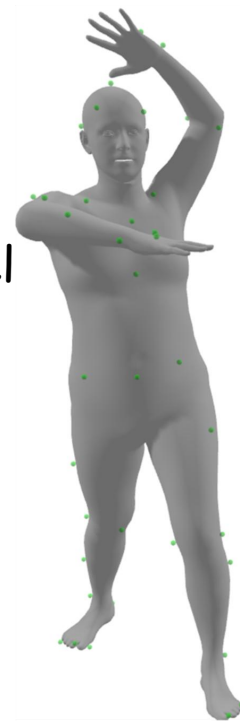
Data Noise n_d

- **Ghost** markers
- **Occluded** markers
- **Measurement Noise**
as random offset to
the markers



Inference Noise n_m

- Automatic Labeling
from previous model





Results THuman



	n_d	n_m	RMSE ↓	MAE ↓	PCK1 ↑	PCK3 ↑	PCK7 ↑
[2, 5]			30.10 <i>mm</i>	3.49°	11.79%	66.85%	98.34%
[20]			30.80 <i>mm</i>	3.10°	12.71%	67.06%	97.71%
Ours (ℓ^m)	✓	✗	28.90 <i>mm</i>	2.98°	14.71%	69.86%	98.18%
Ours ($\ell^m \ell^j$)			23.40 <i>mm</i>	2.29°	19.66%	81.06%	99.11%
[2, 5]			20.60 <i>mm</i>	1.93°	28.71%	89.03%	99.05%
[20]			21.71 <i>mm</i>	1.91°	36.38%	87.75%	98.22%
Ours (ℓ^m)	✗	✓	18.70 <i>mm</i>	1.85°	41.99%	90.95%	98.81%
Ours ($\ell^m \ell^j$)			18.50 <i>mm</i>	1.49°	42.18%	91.44%	98.56%
[2, 5]			23.80 <i>mm</i>	2.03°	24.26%	85.63%	98.22%
[20]			24.87 <i>mm</i>	1.94°	31.99%	84.05%	97.00%
Ours (ℓ^m)	✓	✓	22.40 <i>mm</i>	1.79°	36.01%	87.14%	97.53%
Ours ($\ell^m \ell^j$)			21.90 <i>mm</i>	1.52°	36.67%	88.09%	97.69%

Table 5.2: Noisy landmark fitting on THuman 2.0. Comparison of our noise-aware fitting approach vs. a variant of the fitting method from [2, 5]. RMSE is in meters and PCK in (%). Subscripts j and m denote “joints” and “markers”, while n_d and n_m indicate data and marker noise, respectively.



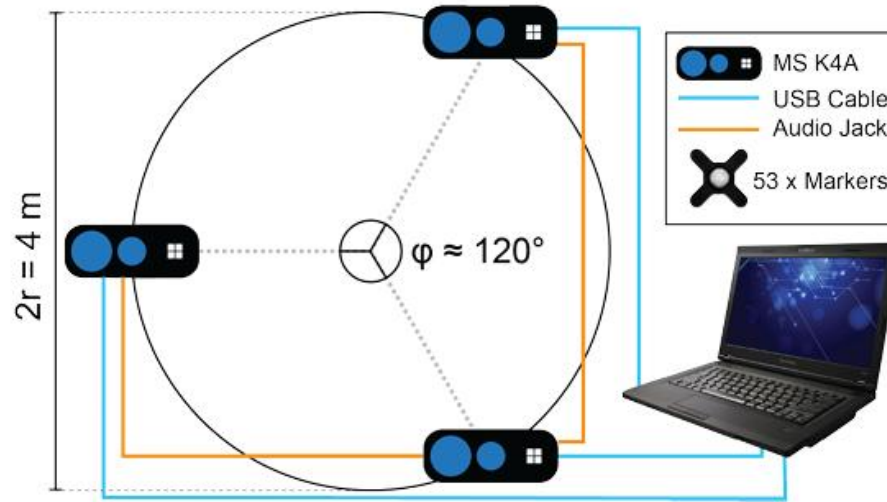


Results vs Mosh++



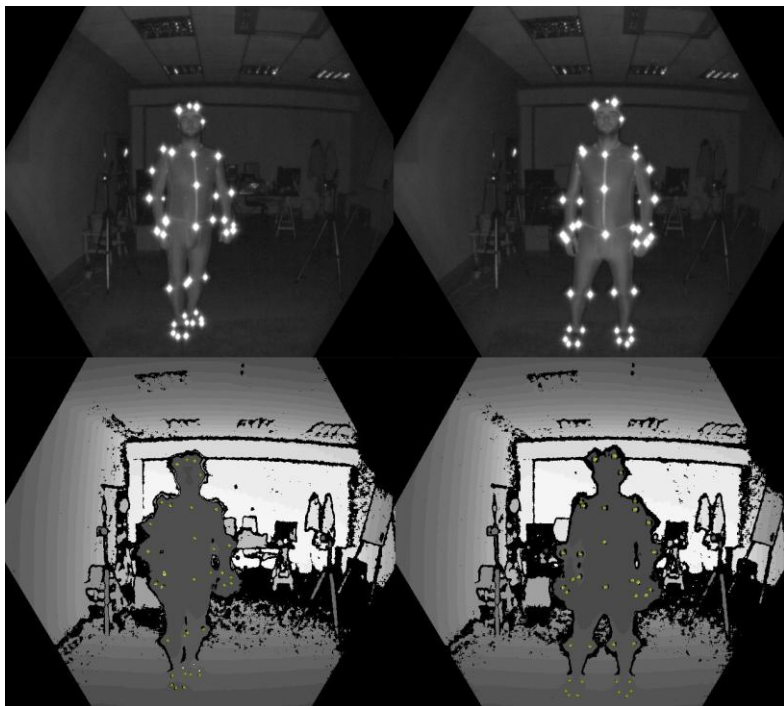


Real-World Deployment





Marker Detection



- Detect Markers in IR



- Ring Around Marker -
→ Centroid → Output:
(x, y, depth) for each
marker → Deproject
to Sensor Space m_n^s





Marker Fusion



~133

Fused in Global Space



-> Cluster ->



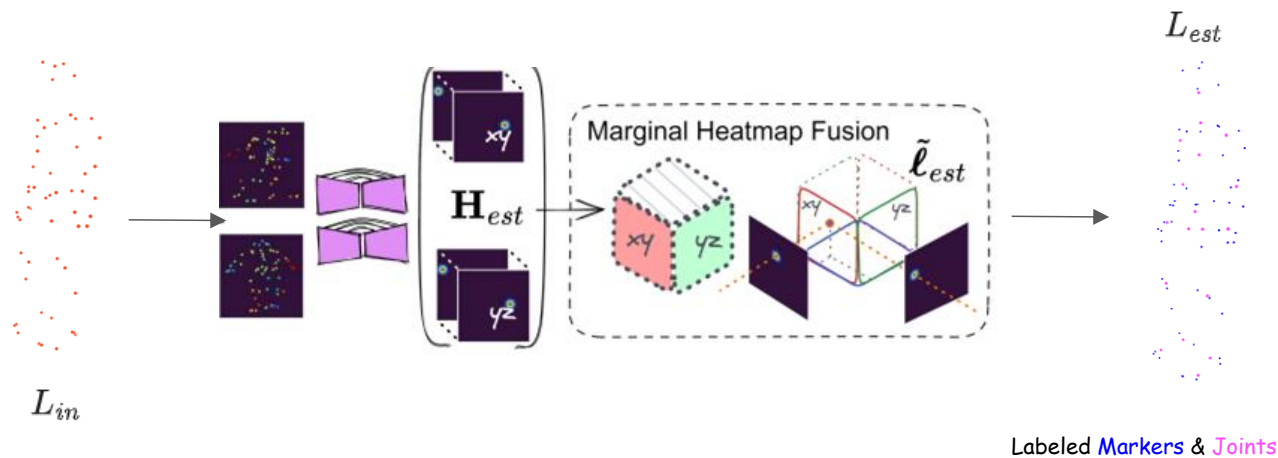
m_n^G

Input Markers~57

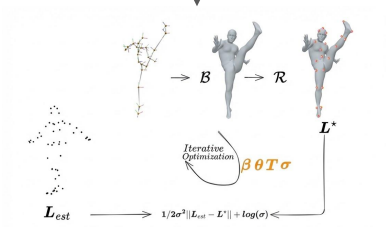




Labelling & Solving



Labeled Markers & Joints

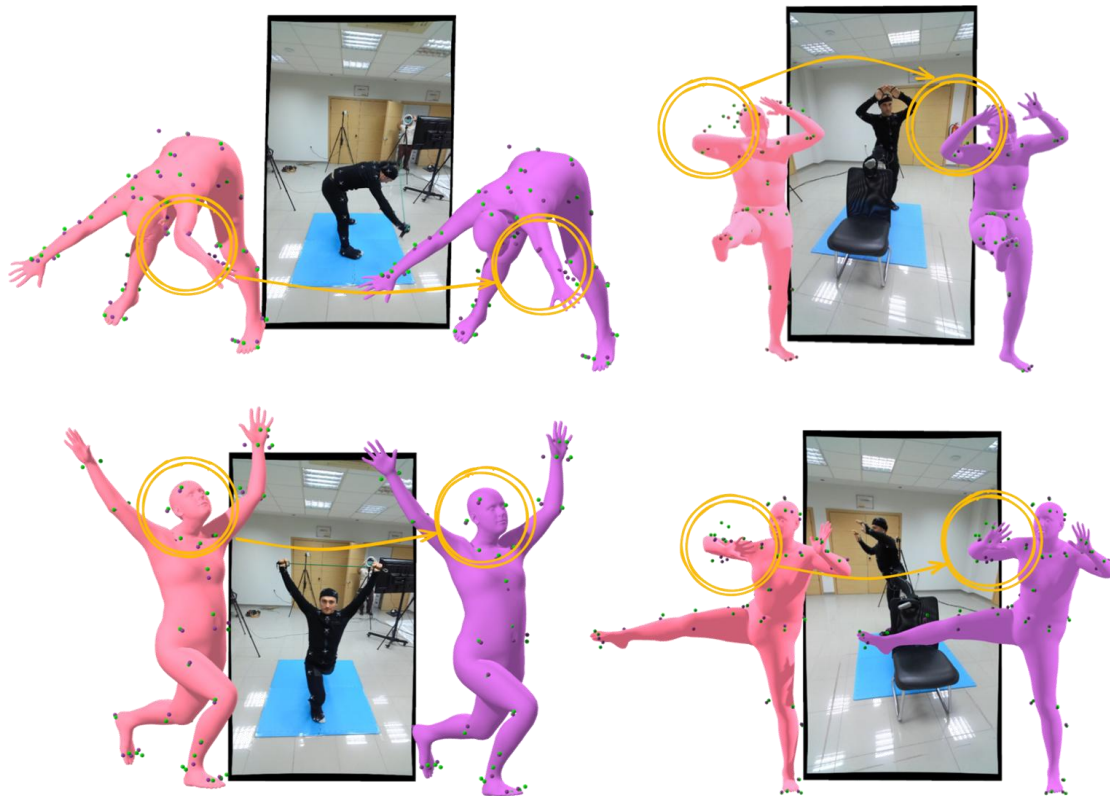


Noise Aware Solver





Ours vs Mosh++





In the wild results



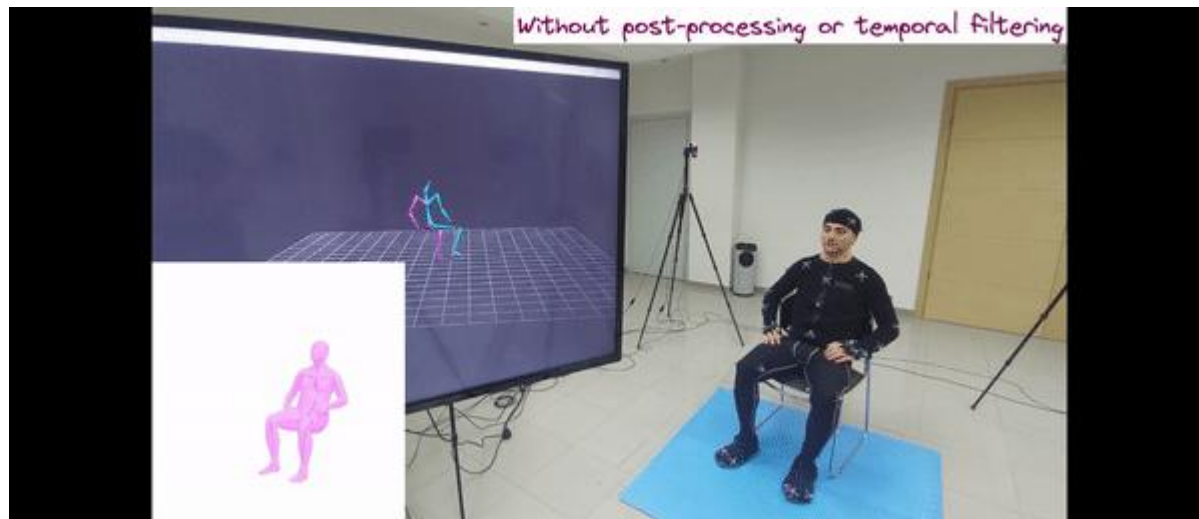
The screenshot displays a motion capture software interface with the following components:

- Blueprint Panel (Left):** A hierarchical tree view showing camera and sensor configurations:
 - depth_cam_0
 - depth_cam_1
 - depth_cam_2
 - depth_cam_3
 - infrared_cam_0
 - predicted
 - pose
 - skeleton
 - rgb_cam_0
 - rgb_cam_1
 - rgb_cam_2
 - rgb_cam_3
 - predicted
 - pose
 - skeleton
 - fitting
 - pose
 - skeleton
- Camera Views (Top and Middle):** Six hexagonal views showing depth maps and skeletal overlays from different camera angles (depth_cam_0, depth_cam_1, depth_cam_2, depth_cam_3).
- RGB View (Middle Right):** A real-world camera view (rgb_cam_0) showing a person in a red and black suit in a room.
- World View (Right):** A 3D rendered view of the person's skeleton in a purple color.
- Timeline (Bottom):** A playback control bar showing "frame_nr", "1.00x", "30 FPS", and "#46". Below it is a "Streams" section with a grid of dots representing data points for various sensors over time.





In the wild results





ICCV Demo



ICCV23

PARIS





Adversary III - Markerless MoCap





Markerless Challenges

- ⚡ High-frequency jitter and sudden changes
- 🚫 Missing key points due to body part occlusions
- 🔄 Flipping body parts
- 🎞️ Inconsistent predictions across adjacent frames

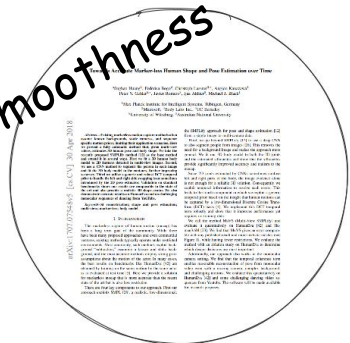




Related Work



DCT smoothness



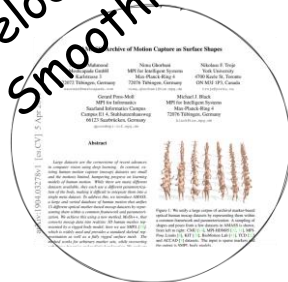
[Huang et al. 2017]

Bundle



[Kanazawa et al. 2019]

Velocity
Smoothness



[Mahmood et al. 2019]

Joints smoothness



[Eye et al. 2022]



[Arnab et al. 2019]



Temporal



Prior constraints



To enforce temporal consistency





Related Work



[Huang et al. 2017]



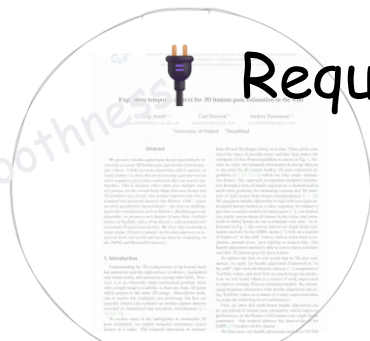
[Kanazawa et al. 2019]



[Mahmood et al. 2019]



[Eye et al. 2022]



[Arnab et al. 2019]

 Time consuming

 Require several Resources

Temporal

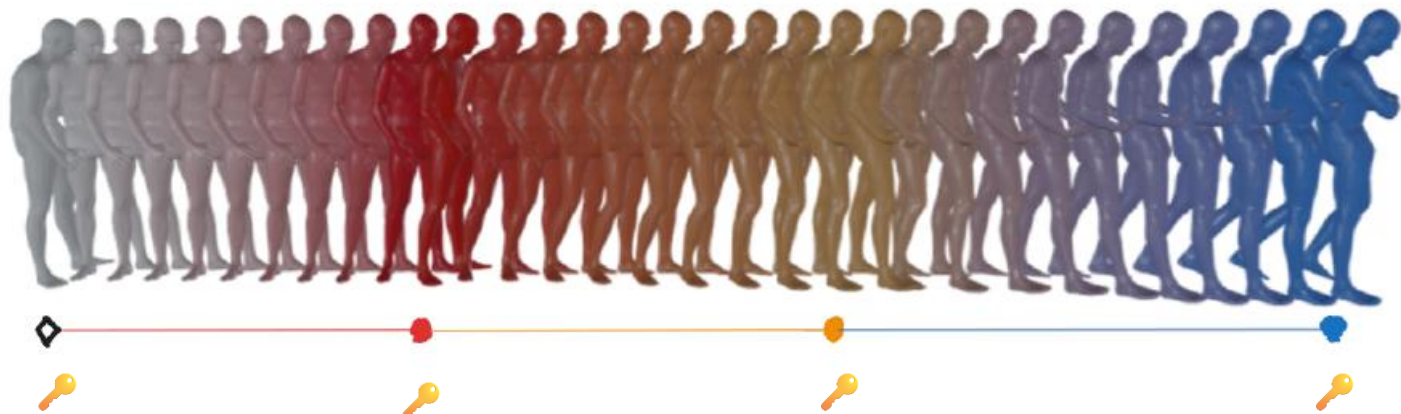
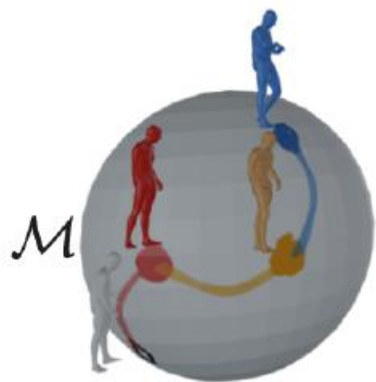
Prior constraints

To enforce temporal consistency





BundleMoCap



- 🔄 Gains robustness to outlier estimates
- 🕒 Produces smooth motions, even without smoothness terms
- ⚡ Maximizes runtime efficiency

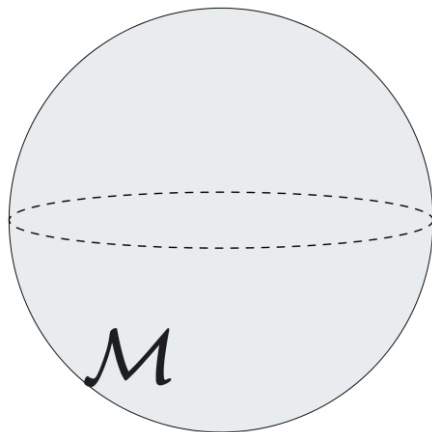




Spherical Human Pose Prior

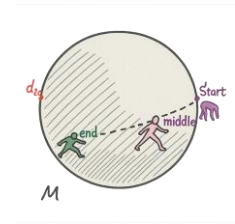
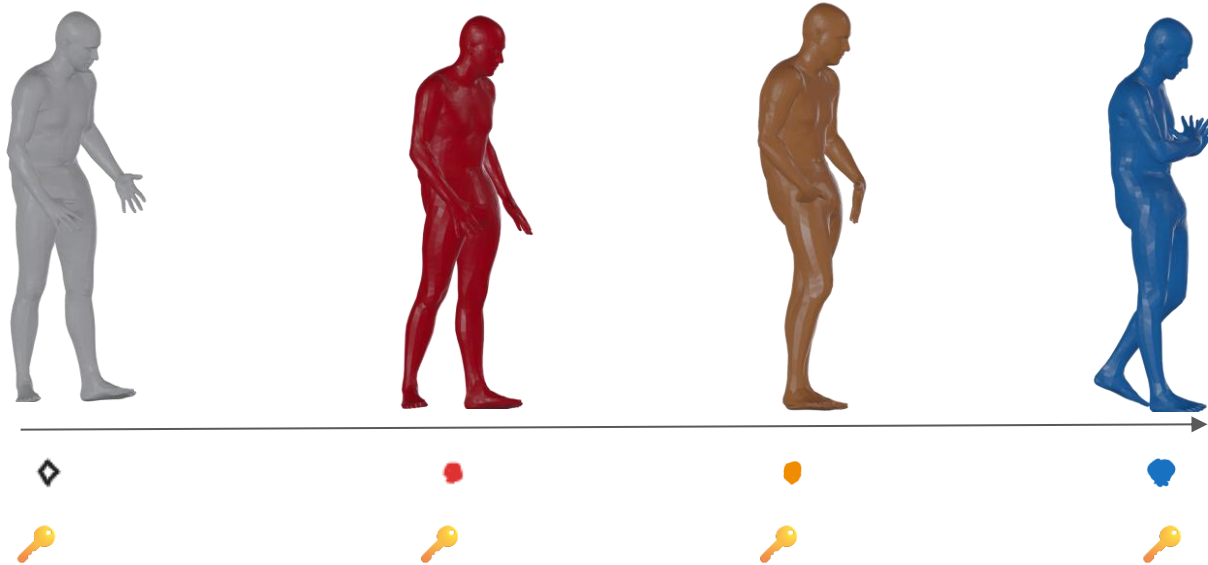


 prior distribution over valid human poses



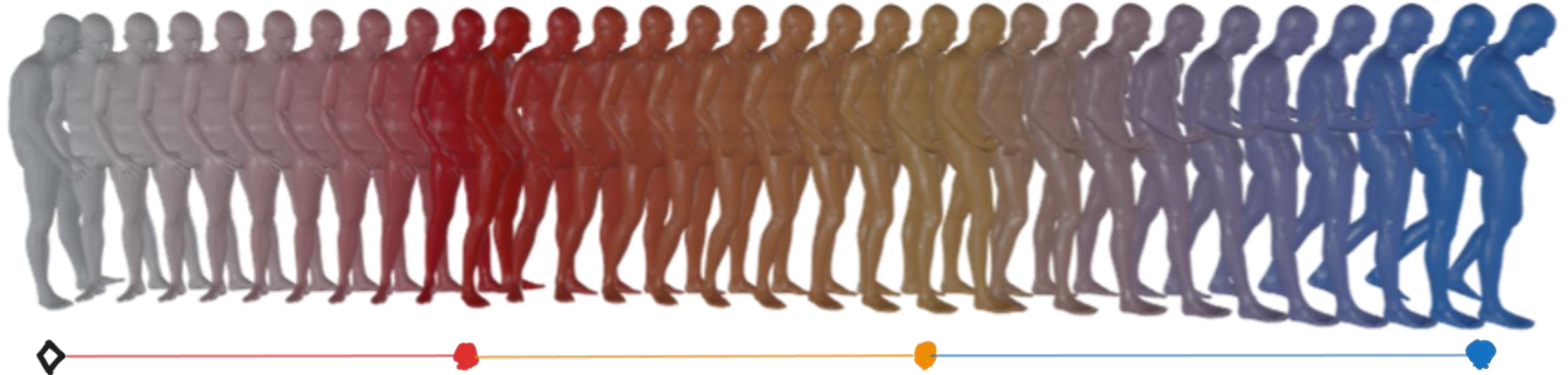


Pose Interpolation



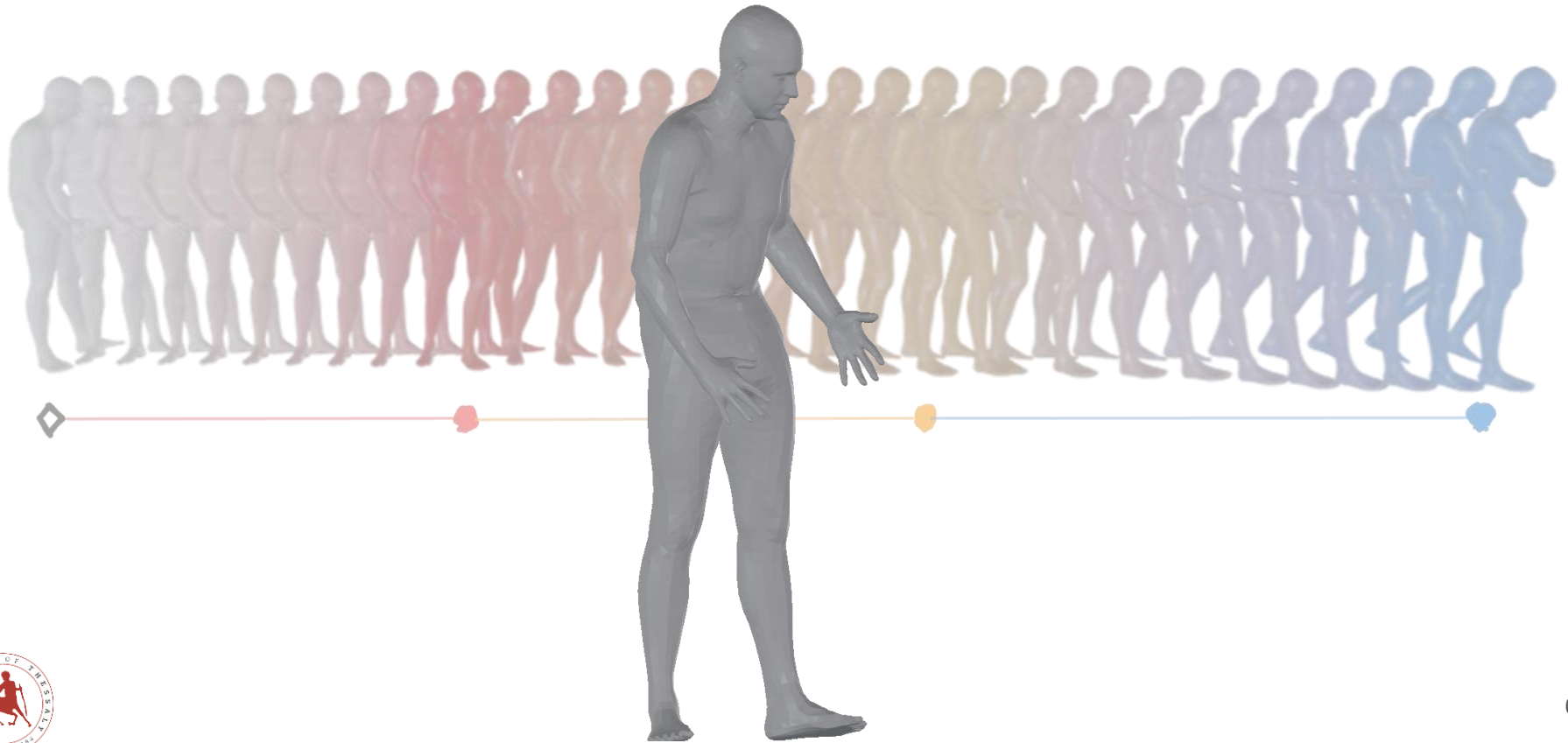


Pose Interpolation





Pose Interpolation





Approach

$$t^1 = 0$$



$$t^1 = T$$



$\mathcal{E}_{prior}^{T^1}$





Approach



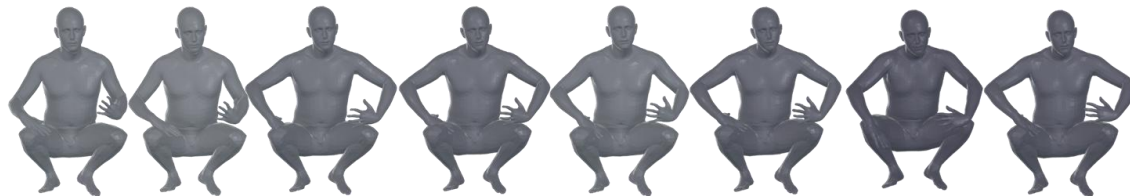
$t^1 = 0$



$t^1 = T$



$$\begin{aligned}\theta^t &= \mathcal{G}(\mathcal{S}^t(z^0, z^{T^1})) \\ \mathcal{R}^t &= \mathcal{S}^t(\mathcal{R}^0, \mathcal{R}^{T^1}) \\ t^t &= \mathcal{L}^t(t^0, t^{T^1})\end{aligned}$$

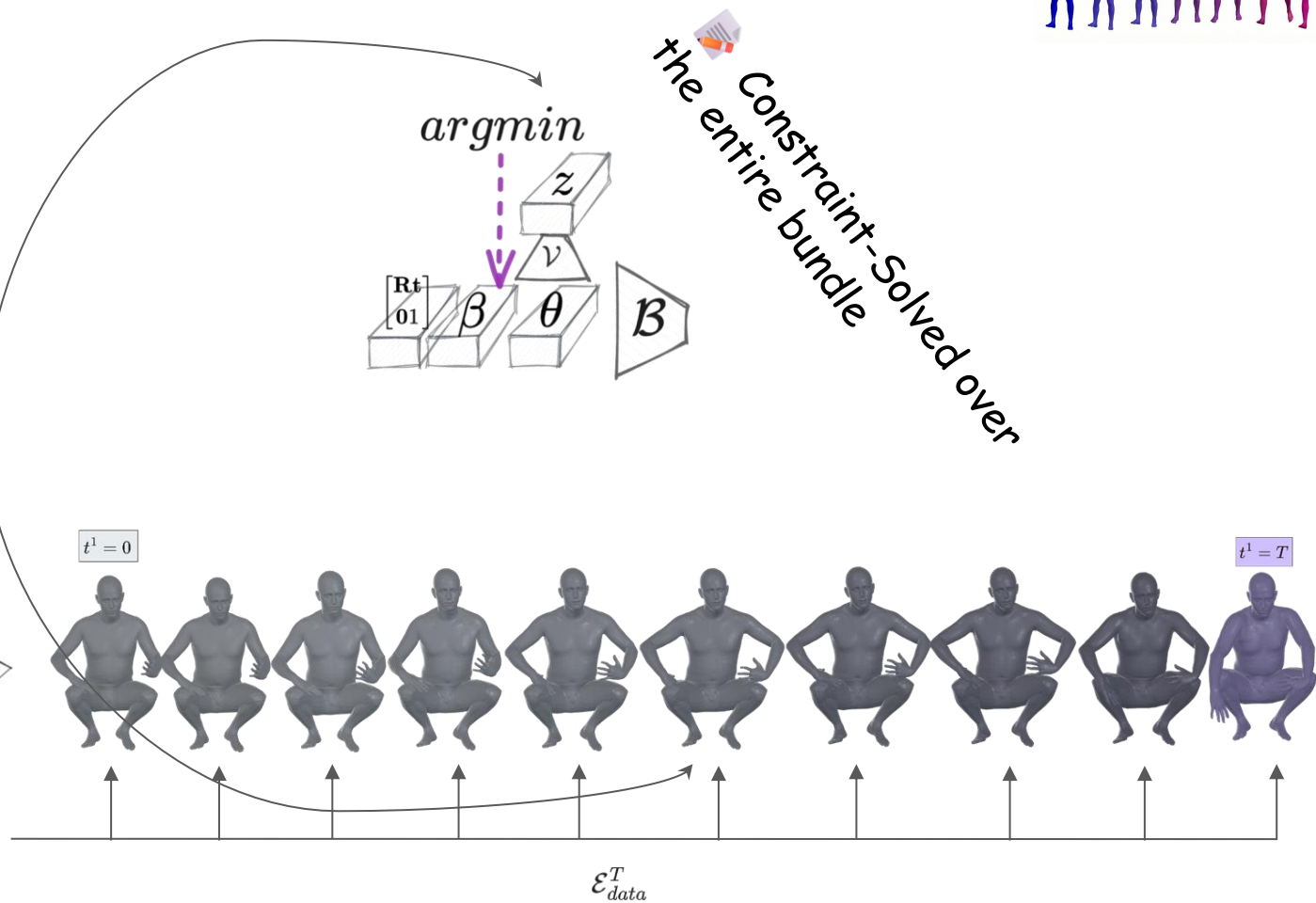
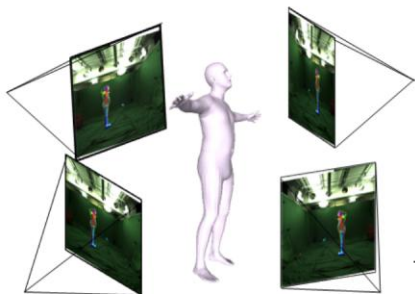




Approach



multi-view 2D
keypoint constraints



Constraint-Solved over
the entire bundle



Sliding Windows

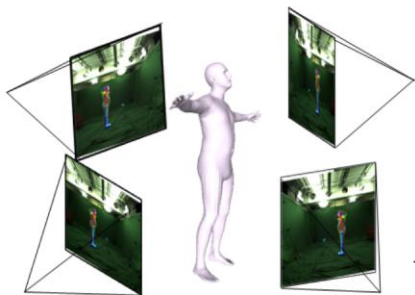


$t^1 = T$

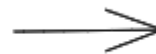


$t^1 = T$

multi-view 2D
keypoint constraints

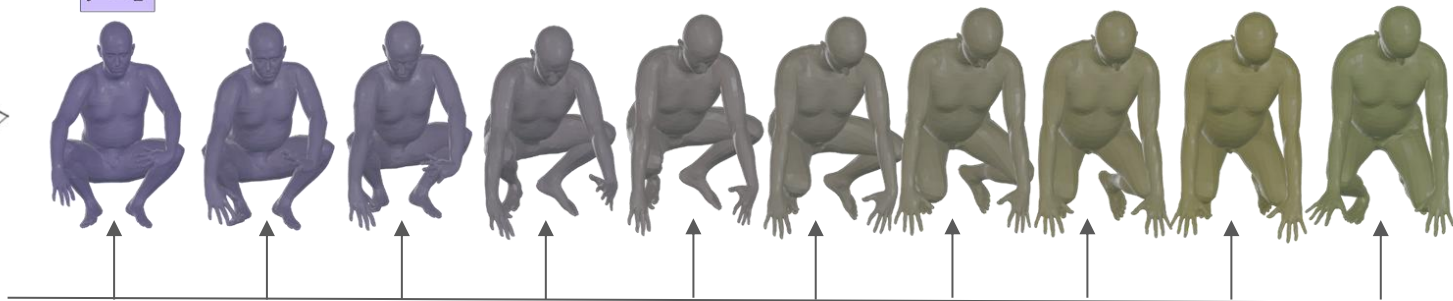


$$\begin{aligned} \theta^t &= \mathcal{G}(\mathcal{S}^t(z^0, z^{T^1})) \\ \mathcal{R}^t &= \mathcal{S}^t(\mathcal{R}^0, \mathcal{R}^{T^1}) \\ t^t &= \mathcal{L}^t(t^0, t^{T^1}) \end{aligned}$$



$\mathcal{E}_{prior}^{T^2}$

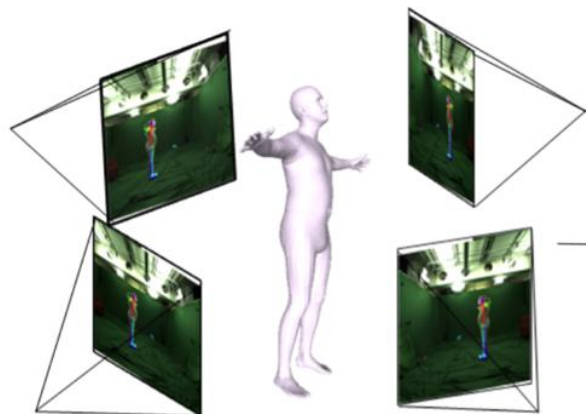
$t^2 = T$



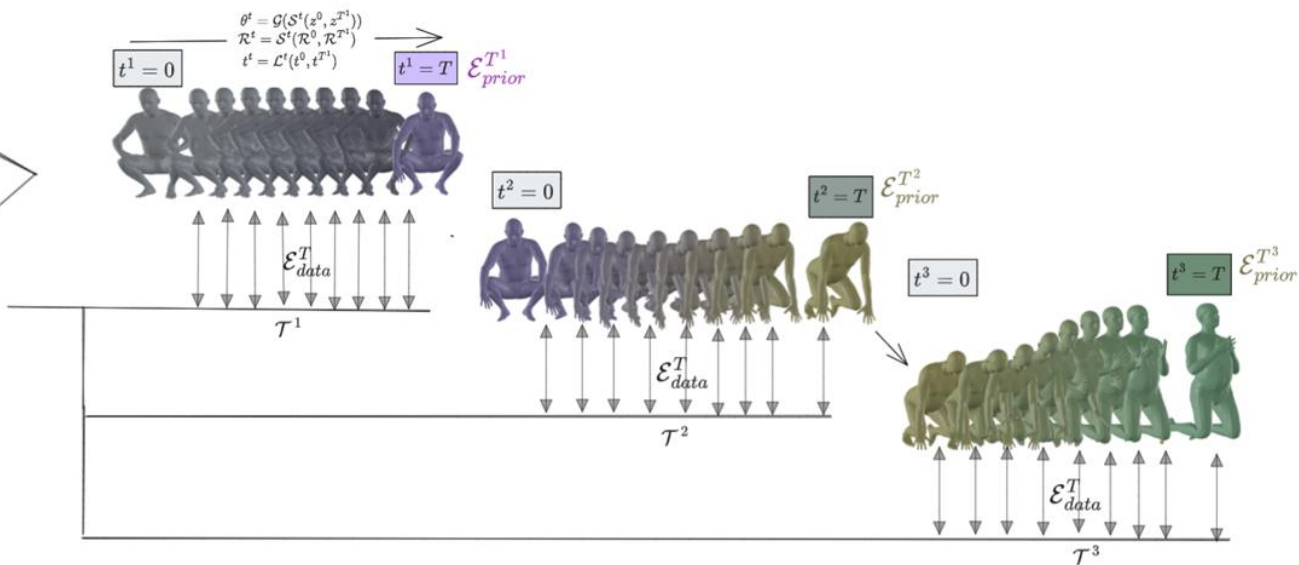
\mathcal{E}_{data}^T



Overview

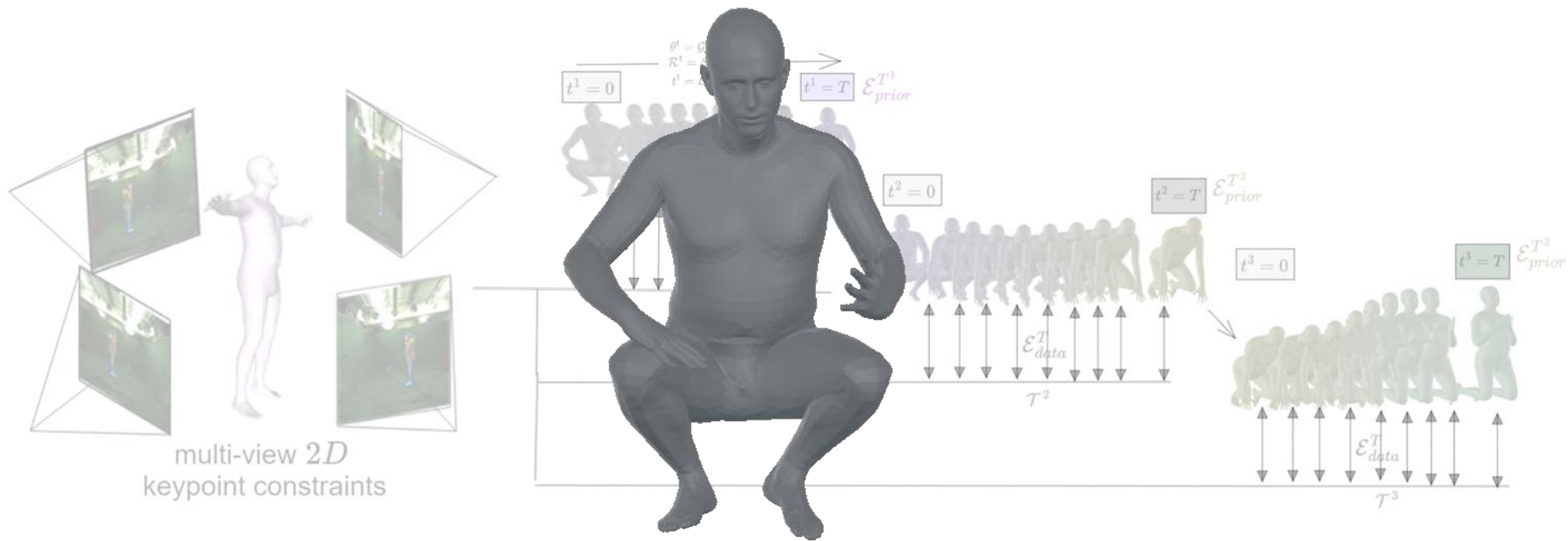


multi-view 2D
keypoint constraints





Overview





Results on standard benchmarks

	MPJPE ↓	RMSE ↓	MAE ↓	PCK3 ↑	PCK7 ↑	accel ↓
<i>MuVS</i>	53.36 <i>mm</i>	58.54 <i>mm</i>	10.23 °	28.02%	79.57%	10.99 <i>mm/s</i> ²
DCT [6]	50.88 <i>mm</i>	56.72 <i>mm</i>	12.32 °	29.21%	80.41%	09.19 <i>mm/s</i> ²
DMMR [9]	60.69 <i>mm</i>	65.16 <i>mm</i>	11.48 °	20.93%	69.48%	09.57 <i>mm/s</i> ²
SLAHMR [10]	50.49 <i>mm</i>	54.52 <i>mm</i>	08.57 °	28.92%	79.20%	09.02 <i>mm/s</i> ²
ETC [7]	72.74 <i>mm</i>	77.83 <i>mm</i>	05.73°	32.63%	84.42%	07.92 <i>mm/s</i> ²
BundleMoCap	38.36 <i>mm</i>	43.10 <i>mm</i>	04.31°	33.70%	86.24%	06.18 <i>mm/s</i> ²
BundleMoCap++	36.32<i>mm</i>	40.93<i>mm</i>	04.11°	46.27%	93.77%	02.52<i>mm/s</i>²

	MPJPE ↓	RMSE ↓	MAE ↓	PCK3 ↑	PCK7 ↑	accel ↓
<i>MuVS</i>	64.99 <i>mm</i>	76.12 <i>mm</i>	6.28°	28.20%	73.75%	14.45 <i>mm/s</i> ²
DCT [6]	62.43 <i>mm</i>	68.13 <i>mm</i>	6.18°	35.84%	83.77%	12.01 <i>mm/s</i> ²
DMMR [9]	57.51 <i>mm</i>	67.66 <i>mm</i>	6.06°	37.52%	81.11%	11.52 <i>mm/s</i> ²
SLAHMR [10]	61.8 <i>mm</i>	62.55 <i>mm</i>	5.74°	40.86%	83.97%	11.34 <i>mm/s</i> ²
ETC [7]	59.51 <i>mm</i>	61.32 <i>mm</i>	5.64°	39.30%	84.50%	10.01 <i>mm/s</i> ²
BundleMoCap	56.41 <i>mm</i>	59.12 <i>mm</i>	5.43°	44.51%	85.71%	07.39 <i>mm/s</i> ²
BundleMoCap ++	48.27 <i>mm</i>	56.44 <i>mm</i>	4.33°	48.75%	89.34%	05.66 <i>mm/s</i>²





Results on standard benchmarks

	MPJPE ↓	RMSE ↓	MAE ↓	PCK3 ↑	PCK7 ↑	accel ↓
<i>MuVS</i>	53.36 mm	58.54 mm	10.23 °	28.02%	79.57%	10.99 mm/s ²
DCT [6]	50.88 mm	56.72 mm	12.32 °	29.21%	80.41%	09.19 mm/s ²
DMMR [9]	60.69 mm	65.16 mm	11.48 °	20.93%	69.48%	09.57 mm/s ²
SLAHMR [10]	50.49mm	54.52 mm	08.57 °	28.92%	79.20%	09.02 mm/s ²
ETC [7]	72.74 mm	77.83 mm	05.73°	32.63%	84.42%	07.92 mm/s ²
BundleMoCap	38.36 mm	43.10 mm	04.31°	33.70%	86.24%	06.18mm/s ²
BundleMoCap++	36.32mm	40.93mm	04.11°	46.27%	93.77%	02.52mm/s²

	MPJPE ↓	RMSE ↓	MAE ↓	PCK3 ↑	PCK7 ↑	accel ↓
<i>MuVS</i>	64.99 mm	76.12 mm	6.28°	28.20%	73.75%	14.45 mm/s ²
DCT [6]	62.43 mm	68.13 mm	6.18°	35.84%	83.77%	12.01 mm/s ²
DMMR [9]	57.51 mm	67.66 mm	6.06°	37.52%	81.11%	11.52 mm/s ²
SLAHMR [10]	61.8 mm	62.55 mm	5.74°	40.86%	83.97%	11.34 mm/s ²
ETC [7]	59.51 mm	61.32 mm	5.64°	39.30%	84.50%	10.01 mm/s ²
BundleMoCap	56.41 mm	59.12 mm	5.43°	44.51%	85.71%	07.39 mm/s ²
BundleMoCap ++	48.27 mm	56.44 mm	4.33°	48.75%	89.34%	05.66 mm/s²





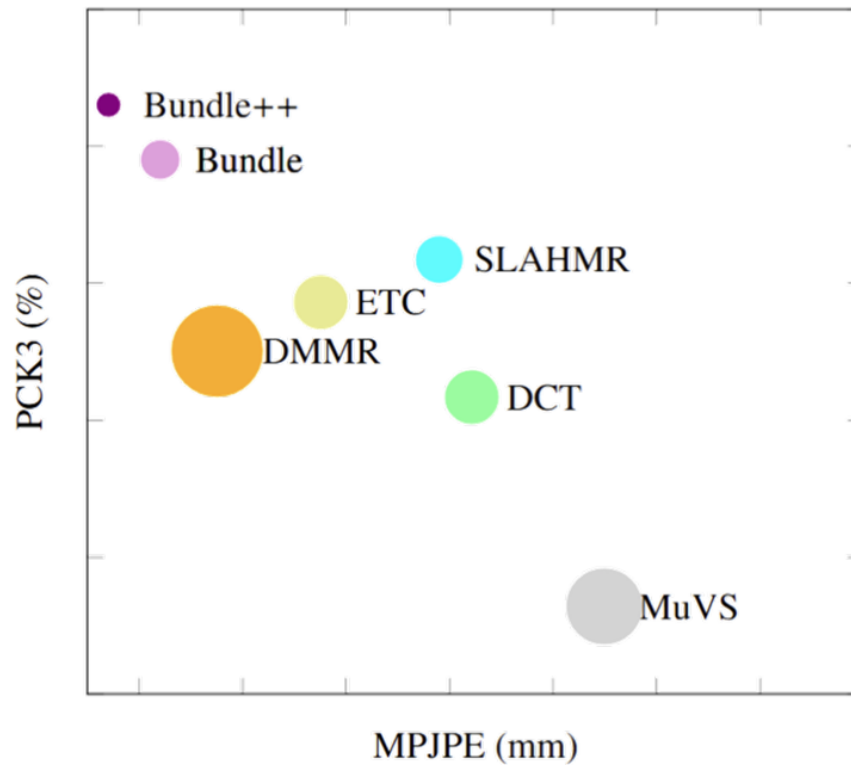
Realism of the provided motion

	FS ↓
<i>MuVS</i>	0.09 <i>cm/f</i>
DCT	0.09 <i>cm/f</i>
DMMR	0.06 <i>cm/f</i>
SLAHMR	0.07 <i>cm/f</i>
ETC	0.06 <i>cm/f</i>
BundleMoCap	0.07 <i>cm/f</i>
BundleMoCap++	0.03 <i>cm/f</i>





Performance vs Efficiency





VAE Quality

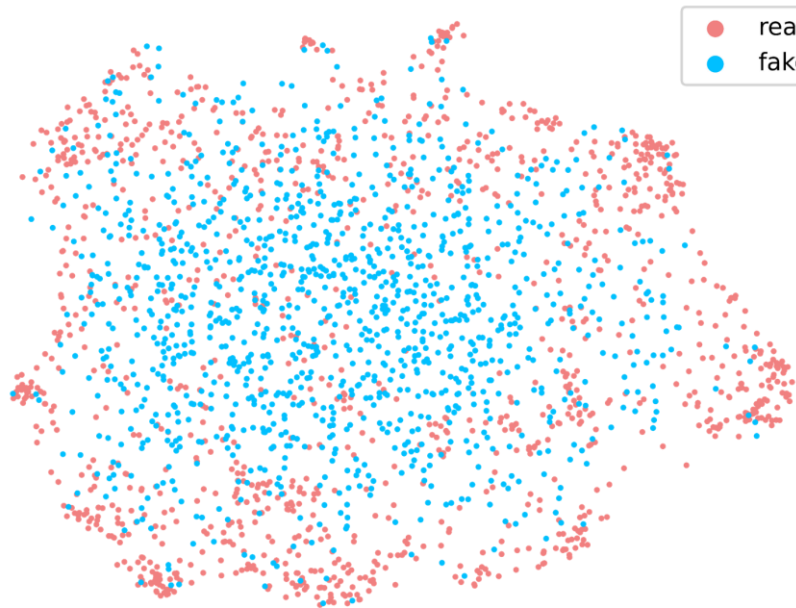


	Synthesis		Reconstruction		
	FID ↓	DIV ↑	MPJPE ↓	PCK3 ↑	PCK7 ↑
VPoser	9.94	12.11	26.21mm	62.33%	89.82%
RVPoser	8.57	13.24	24.91mm	70.01%	94.05%
LieVAE	14.55	13.20	32.45 mm	55.32%	85.65%
SVAE	12.22	19.51	27.81 mm	66.14%	91.07%
SPoser(ours)	3.45	18.12	24.88 mm	69.67%	93.99%

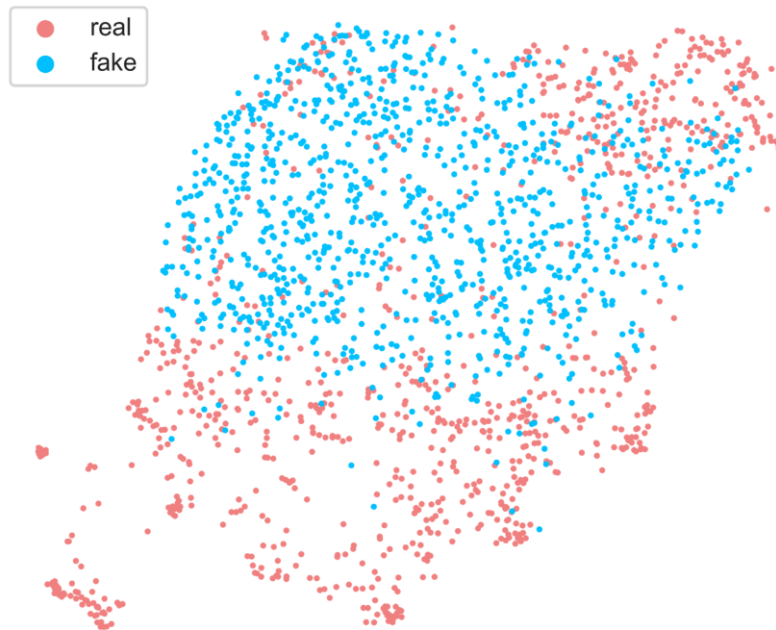




VAE Quality



SPoser

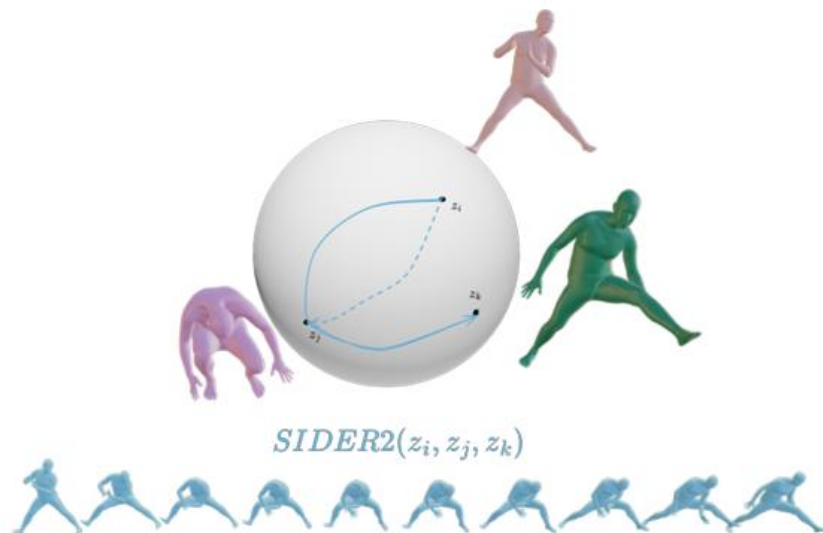


VPoser



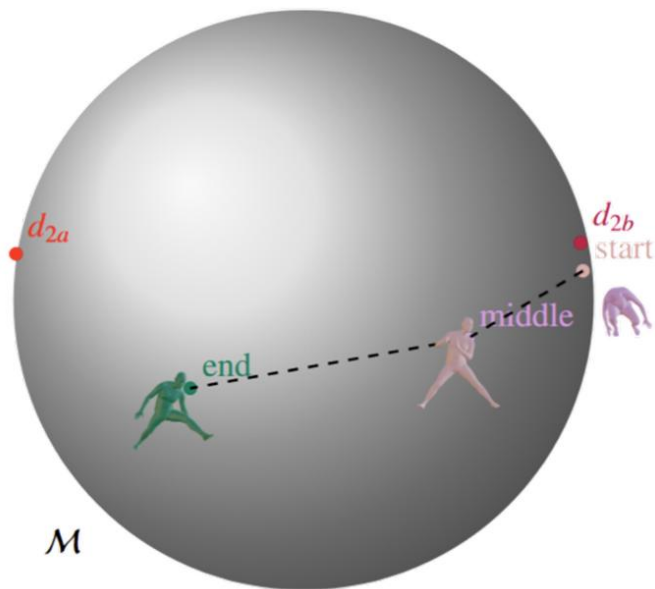


VAE Quality





SIDER Interpolation



then

$$\mathbf{d}_{2a} = \text{SLERP}(\mathbf{q}_3, \mathbf{q}_2, 2), \quad \mathbf{d}_{2b} = \text{SLERP}(\mathbf{q}_1, \mathbf{q}_2, 2),$$

$$\mathbf{c}_{inner} = \text{SLERP}(\mathbf{q}_1, \mathbf{d}_{2a}, t), \quad \mathbf{c}_{outer} = \text{SLERP}(\mathbf{d}_{2b}, \mathbf{q}_3, t),$$

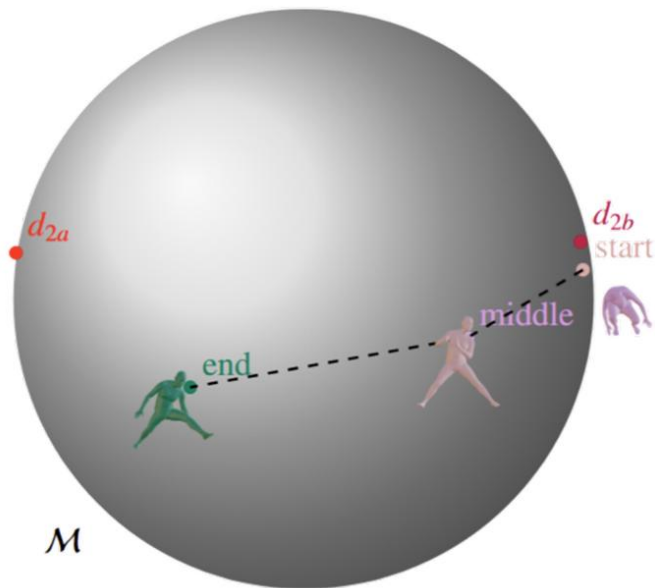
and finally

$$\text{SIDER2}(\mathbf{q}_1, \mathbf{q}_2, \mathbf{q}_3, t) = \text{SLERP}(\mathbf{c}_{inner}, \mathbf{c}_{outer}, t).$$





SIDER vs SLEPR

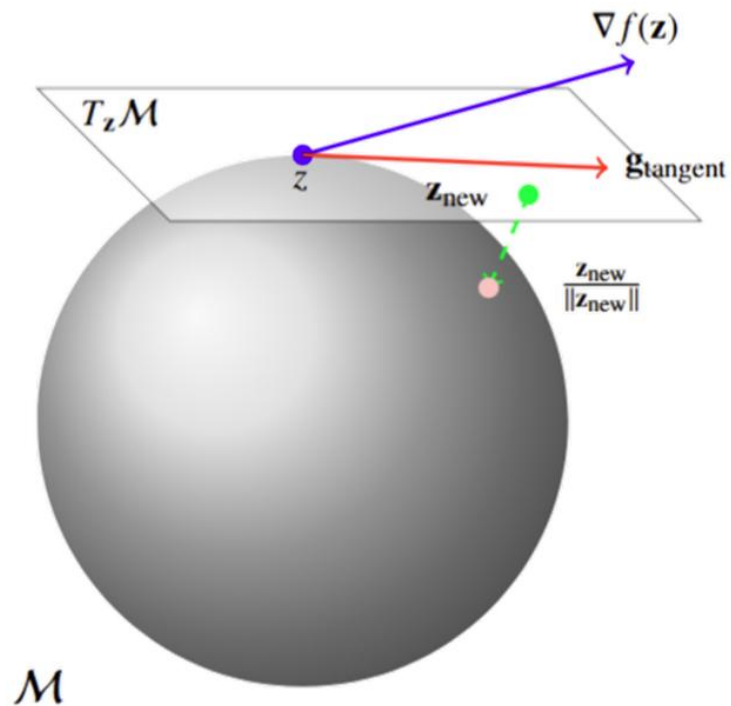


	MPJPE ↓	RMSE ↓	MAE ↓	PCK3 ↑	PCK7 ↑	accel ↓
<i>SLEPR</i>	37.82 mm	42.62 mm	04.15°	35.86%	86.94%	3.66 mm/s ²
<i>SIDER2</i>	36.32 mm	40.93 mm	04.09°	46.27%	93.97%	02.52 mm/s²



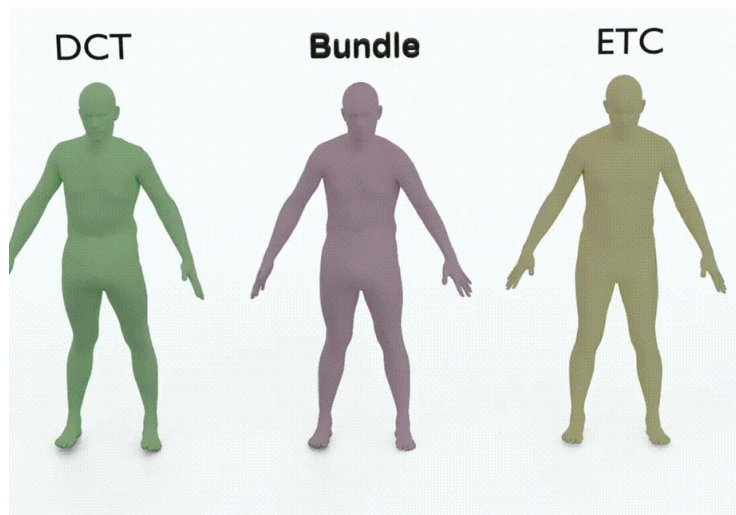


Optimisation upon the manifold

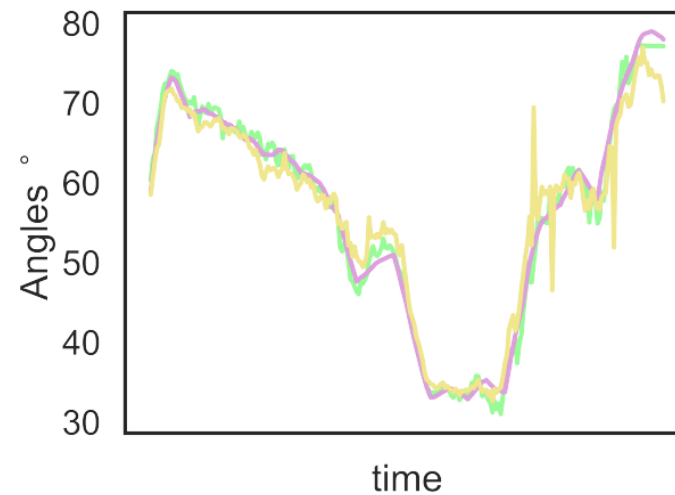




Smoothness

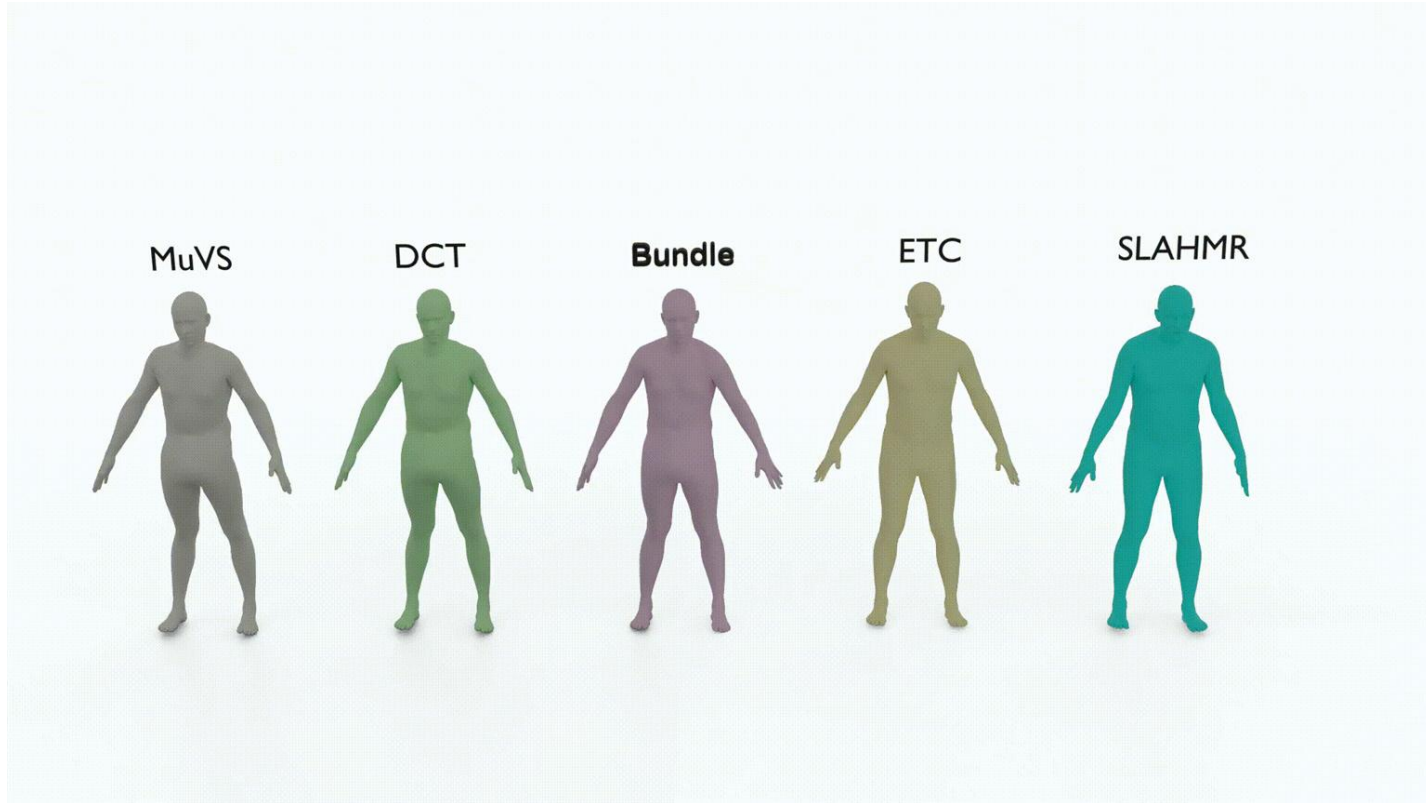


Knee flexion





Comparisons





Comparisons vs Pose Estimators

	MPJPE ↓	RMSE ↓	PCK3 ↑	PCK7 ↑	accel ↓
MVN [14]	85.34 <i>mm</i>	114.03 <i>mm</i>	10.76%	62.48%	07.45 <i>mm/s²</i>
BundleMoCap++	48.27 <i>mm</i>	56.44 <i>mm</i>	48.75%	89.34%	05.34 <i>mm/s²</i>

MPI-INF-3DHP





Comparisons vs Monocular

	MPJPE ↓	PAMPJPE ↓	RMSE ↓	MAE ↓	PCK3 ↑	PCK7 ↑	accel ↓
<i>H4D</i>		49.05 mm	56.70 mm	7.56°	40.34%	82.35%	18.10 mm/s ²
<i>TCMR</i>		110.4 mm	135.4 mm	15.56°	10.94%	55.46%	10.70 mm/s ²
BundleMoCap++	48.27 mm		56.44 mm	4.33°	48.75%	89.34%	05.66 mm/s ²

MPI-INF-3DHP





Comparisons vs Monocular

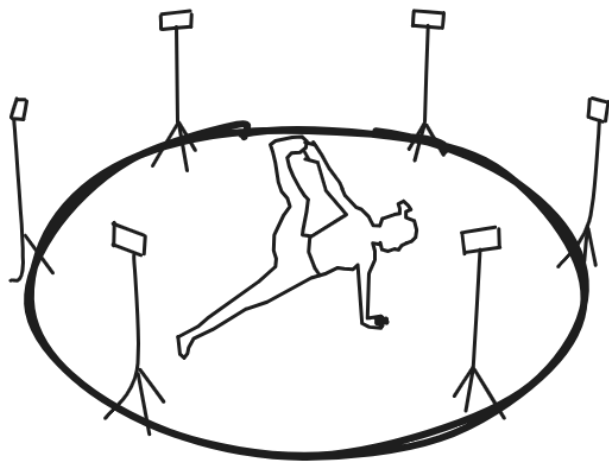
	MPJPE ↓	PAMPJPE ↓	RMSE ↓	MAE ↓	PCK3 ↑	PCK7 ↑	accel ↓
<i>H4D</i>		49.05 mm	56.70 mm	7.56°	40.34%	82.35%	18.10 mm/s ²
<i>TCMR</i>		110.4 mm	135.4 mm	15.56°	10.94%	55.46%	10.70 mm/s ²
BundleMoCap++	48.27 mm		56.44 mm	4.33°	48.75%	89.34%	05.66 mm/s ²

MPI-INF-3DHP





Low-cost setup results



📷 8x (calibrated & synchronised sensors)

🎞️ ⌚ 60 fps

💻 1920x1080



Low-cost setup results





CVMP Demo

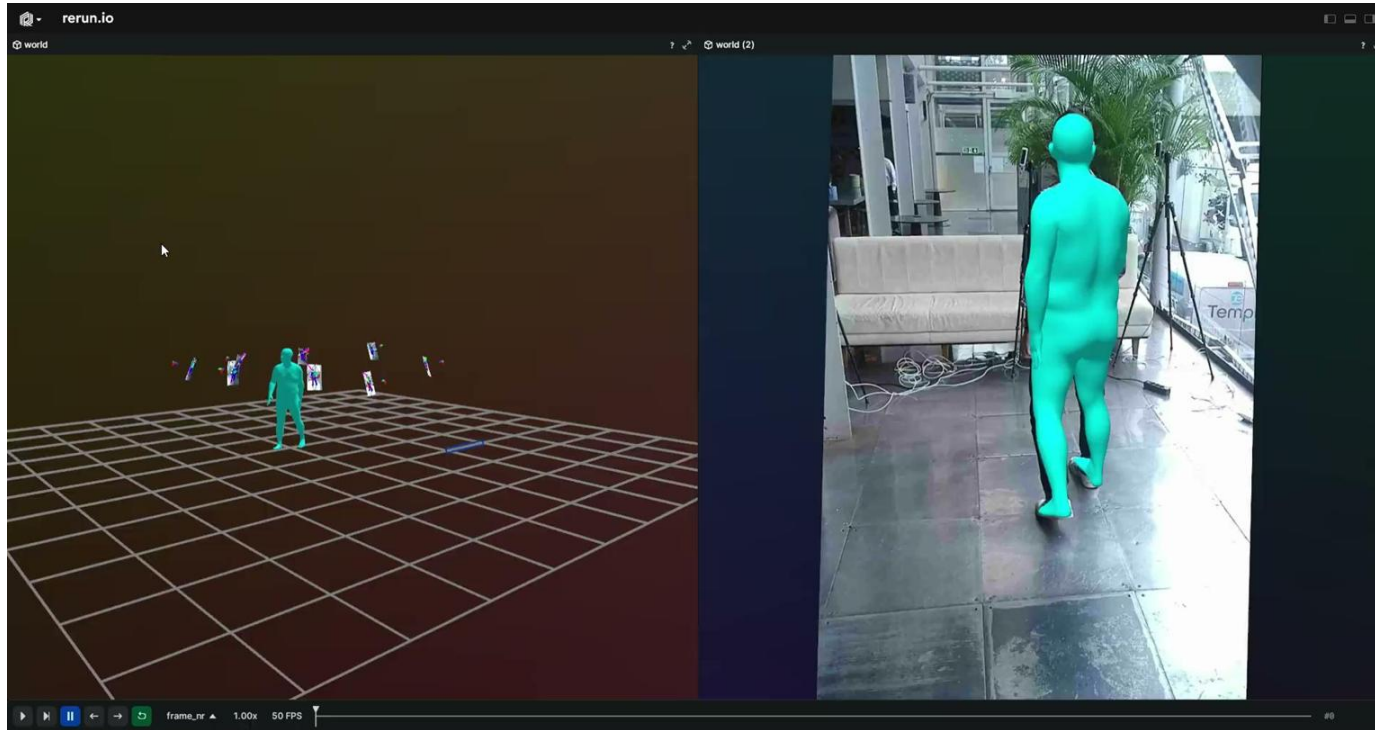


CVMP2023





CVMP Demo





Scientific Publications

Towards Scalable and Real-time
Markerless Motion Capture.



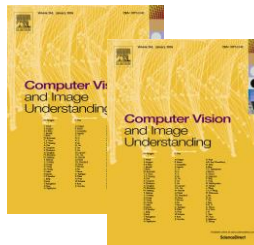
Noise-in, Bias-out: Balanced and Real-time
MoCap Solving



BundleMoCap: Efficient, Robust and
Smooth Motion Capture from Sparse
Multiview Videos.



BundleMoCap++: Efficient, Robust and
Smooth Motion Capture from Sparse Multi
view Videos.



From bias to balance: Leverage
representation learning for bias-free
MoCap solving

Robust and Efficient AI Motion Capture





Scientific Demos



MoCatalyst: Accelerating and Automating
MoCap

ICCV23
PARIS

LightMoCap: Light-weight,
Real-time and Scalable Markerless Motion
Capture

 **CVMP**2023

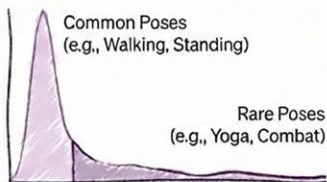




Summary

Representation learning to solve real-world problems around MoCap

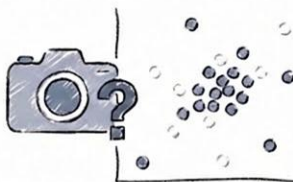
Adversary I: Data Bias



The Problem: Datasets are dominated by walking and standing. Complex poses (yoga, combat) are statistically ignored.

The Solution: Representation Learning & Rare-Pose Synthesis.

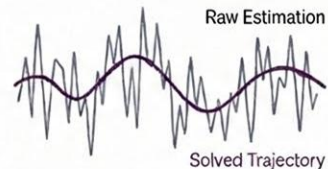
Adversary II: Compound Noise



The Problem: Low-cost sensors introduce noise, which combined with information noise from the AI model is difficult to handle.

The Solution: Uncertainty-Aware Neural Solvers.

Adversary III: Markerless MoCap



The Problem: Frame-by-frame estimation lacks continuity, leading to shaking and sliding.

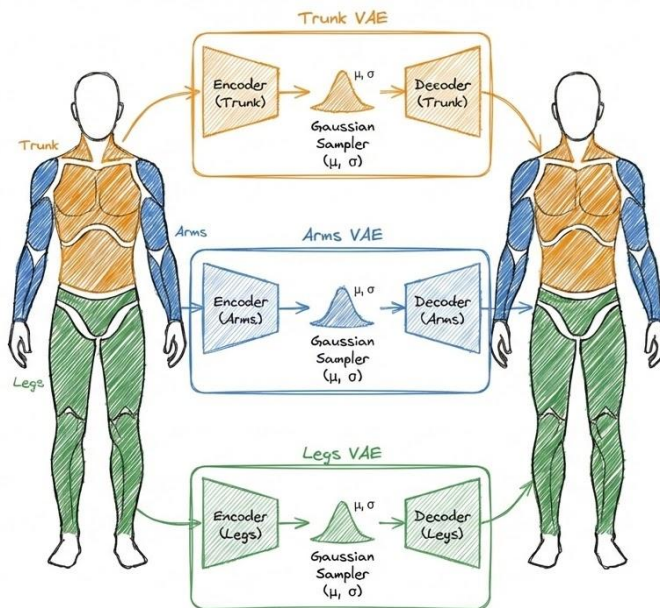
The Solution: Hyperspherical Manifolds & Bundle Solving.





Future Investigation

- Disentangled VAE \rightarrow Better Representations (SO3)





Future Investigation



- Bundle Fingers





Future Investigation

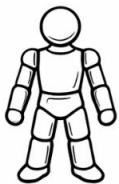


- Towards implicit representations

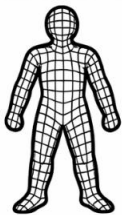




Stickman



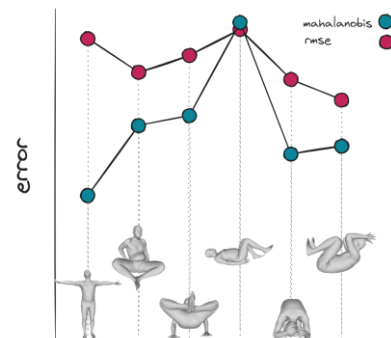
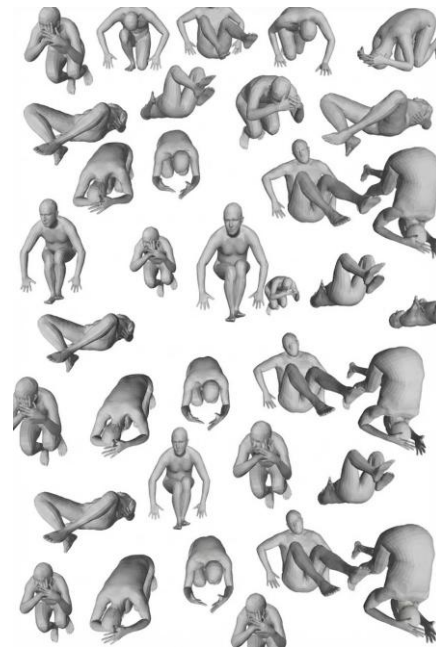
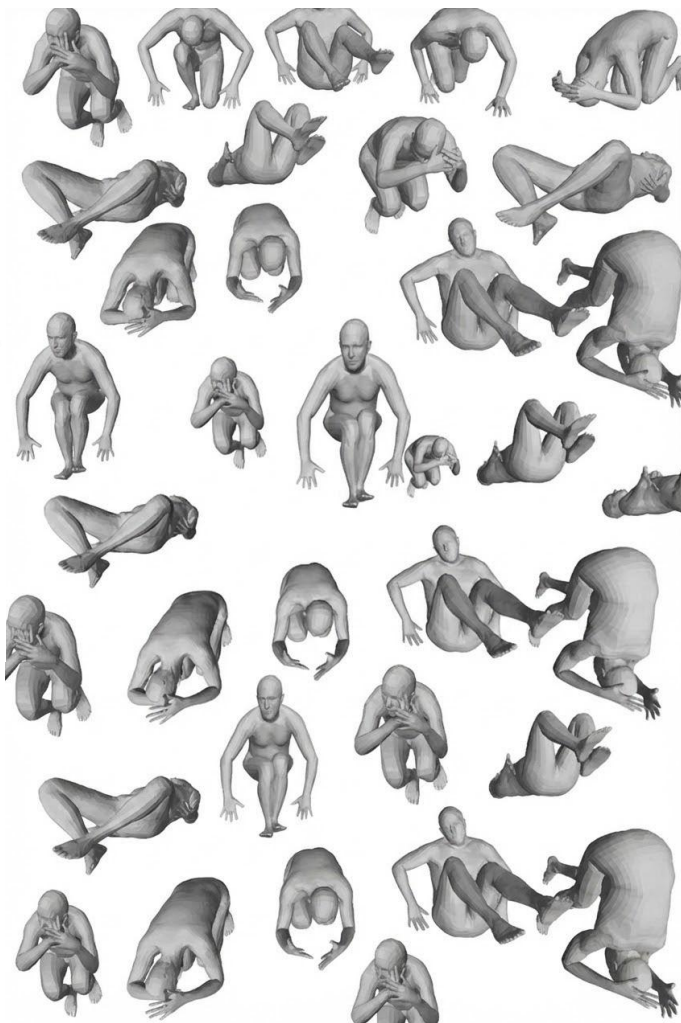
Primitive Based



Mesh-Based



Implicit



Thank you



"Nothing happens until something moves" - Albert Einstein

Candidate: Georgios Albanis, Supervisor: Dr. Konstantinos Kolomvatsos

